The Plant Cell, Vol. 26: 894–914, March 2014, www.plantcell.org

LARGE-SCALE BIOLOGY ARTICLE

Complete Proteomic-Based Enzyme Reaction and Inhibition Kinetics Reveal How Monolignol Biosynthetic Enzyme Families Affect Metabolic Flux and Lignin in *Populus trichocarpa*[W]

Jack P. Wang,[a,b] Punith P. Naik,[c] Hsi-Chuan Chen,[b] Rui Shi,[b] Chien-Yuan Lin,[b] Jie Liu,[b] Christopher M. Shuford,[b] Quanzi Li,[a,b,d] Ying-Hsuan Sun,[e] Sermsawat Tunlaya-Anukit,[b] Cranos M. Williams,[f] David C. Muddiman,[g] Joel J. Ducoste,[c] Ronald R. Sederoff,[b] and Vincent L. Chiang[a,b,h,1]

[a] State Key Laboratory of Tree Genetics and Breeding, Northeast Forestry University, Harbin 150040, China
[b] Forest Biotechnology Group, Department of Forestry and Environmental Resources, North Carolina State University, Raleigh, North Carolina 27695
[c] Civil, Construction, and Environmental Engineering, North Carolina State University, Raleigh, North Carolina 27695
[d] College of Forestry, Shandong Agricultural University, Taian, Shandong 271018, China
[e] Department of Forestry, National Chung-Hsing University, Taichung, 40227, Taiwan
[f] Electrical and Computer Engineering, North Carolina State University, Raleigh, North Carolina 27695
[g] W.M. Keck FT-ICR Mass Spectrometry Laboratory, Department of Chemistry, North Carolina State University, Raleigh, North Carolina 27695
[h] Department of Forest Biomaterials, North Carolina State University, Raleigh, North Carolina 27695

ORCID IDs: 0000-0002-5392-0076 (J.P.W.); 0000-0002-7152-9601 (V.L.C.)

We established a predictive kinetic metabolic-flux model for the 21 enzymes and 24 metabolites of the monolignol biosynthetic pathway using *Populus trichocarpa* secondary differentiating xylem. To establish this model, a comprehensive study was performed to obtain the reaction and inhibition kinetic parameters of all 21 enzymes based on functional recombinant proteins. A total of 104 Michaelis-Menten kinetic parameters and 85 inhibition kinetic parameters were derived from these enzymes. Through mass spectrometry, we obtained the absolute quantities of all 21 pathway enzymes in the secondary differentiating xylem. This extensive experimental data set, generated from a single tissue specialized in wood formation, was used to construct the predictive kinetic metabolic-flux model to provide a comprehensive mathematical description of the monolignol biosynthetic pathway. The model was validated using experimental data from transgenic *P. trichocarpa* plants. The model predicts how pathway enzymes affect lignin content and composition, explains a long-standing paradox regarding the regulation of monolignol subunit ratios in lignin, and reveals novel mechanisms involved in the regulation of lignin biosynthesis. This model provides an explanation of the effects of genetic and transgenic perturbations of the monolignol biosynthetic pathway in flowering plants.

INTRODUCTION

Lignin is a phenolic polymer entangled covalently with cellulose and hemicelluloses in the secondary cell walls of vascular plants (Sarkanen and Ludwig, 1971; Boerjan et al., 2003; Ralph et al., 2007) and plays a critical role in vascular transport and mechanical support (Harada and Cote, 1985). Lignin polymer is composed of three major subunits, guaiacyl (G), syringyl (S), and 4-hydroxyphenyl (H) components (Sarkanen and Ludwig, 1971; Terashima et al., 2009). These subunits are derived from three corresponding monolignols: coniferyl alcohol for G subunits, sinapyl alcohol for S subunits, and 4-hydroxycoumaryl alcohol for H subunits. Lignin composition is typically characterized by the type of subunits and their ratios. In conifers, lignin is predominantly composed of G subunits with a minor fraction of H subunits. In woody dicotyledons, such as *Populus trichocarpa*, lignin is polymerized from mostly G and S subunits with an S/G ratio of 2 (Brown, 1961; Higuchi and Brown, 1963; Sarkanen and Ludwig, 1971).

Research on the biosynthesis of H, G, and S monolignols has been long-standing and extensive (Freudenberg et al., 1952; Wright et al., 1958; Brown, 1961; Higuchi and Brown, 1963). Ten enzyme families convert Phe to these monolignols (Higuchi, 1997; Shi et al., 2010; Figure 1). The resulting supply and ratios of monolignols controlled by the metabolic-flux distributions determine lignin composition, content, and structure (Sederoff et al., 1999; van Parijs et al., 2010). These lignin properties are

[1] Address correspondence to vchiang@ncsu.edu.
The author responsible for distribution of materials integral to the findings presented in this article in accordance with the policy described in the Instructions for Authors (www.plantcell.org) is: Vincent L. Chiang (vchiang@ncsu.edu).
[W] Online version contains Web-only data.
www.plantcell.org/cgi/doi/10.1105/tpc.113.120881

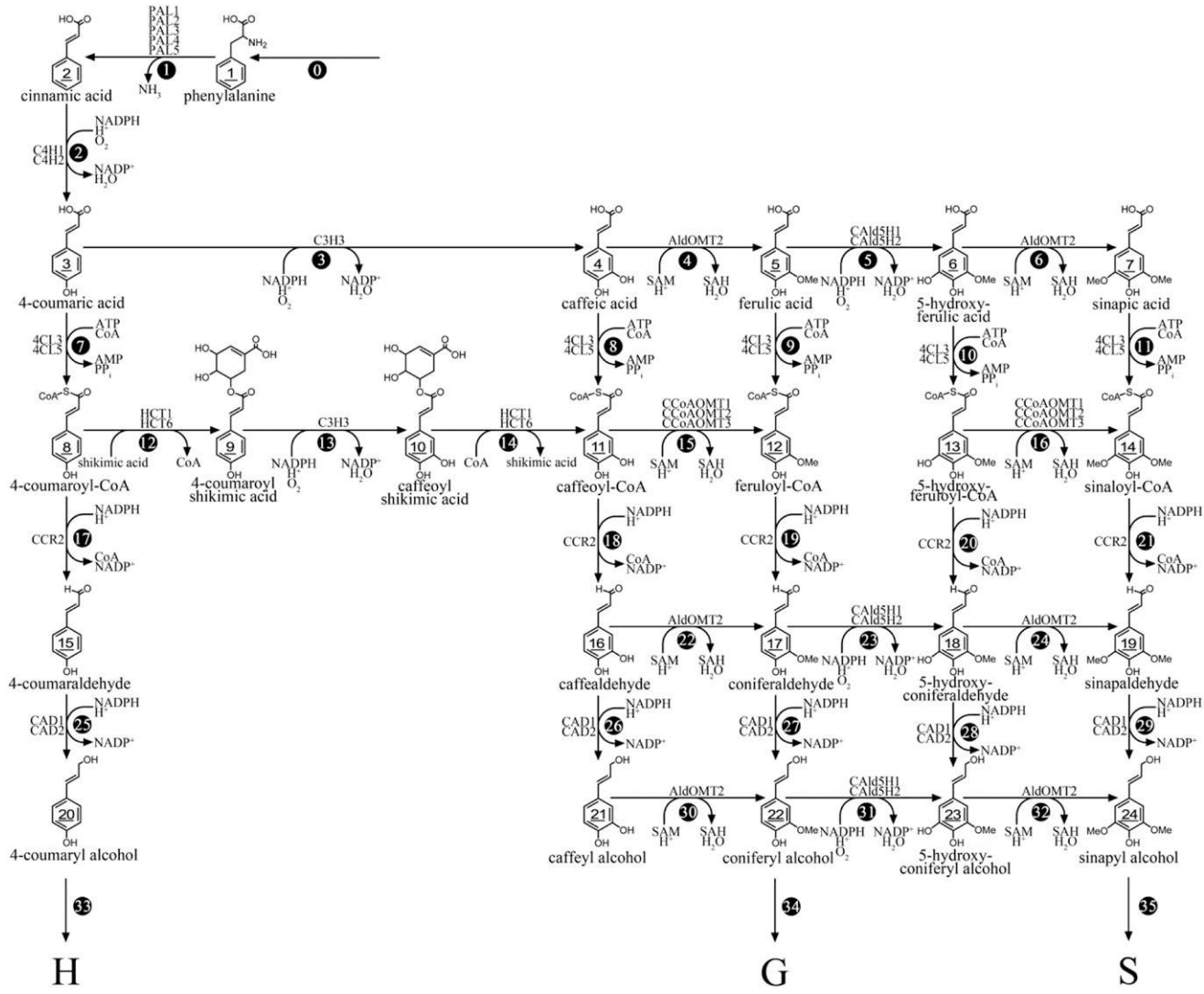

Figure 1. The Monolignol Biosynthetic Pathway in *P. trichocarpa*.

Thirty-five metabolic fluxes (V0 to V35, represented by the circled numbers) mediate the conversion of 24 metabolites (underlined numbers) for monolignol synthesis by the 21 pathway enzymes. First, the deamination of Phe to cinnamic acid is catalyzed by five isoforms of phenylalanine ammonia-lyase (PAL1 to PAL5). Cinnamic acid is then hydroxylated to 4-coumaric acid and subsequently to caffeic acid by a multiple-protein complex of C4H and C3H (Chen et al., 2011). There are two isoforms of C4H (C4H1 and C4H2) and one of C3H (C3H3). Two isoforms of 4-coumaric acid:CoA ligase (4CL3 and 4CL5) activate the hydroxycinnamic acids to their corresponding CoA-thioesters. A cooperative interaction between the C4H-C3H protein complex and two isoforms of hydroxycinnamoyl-CoA shikimate hydroxycinnamoyl transferase (HCT1 and HCT6), hydroxylate 4-coumaroyl-CoA at the ring-3 position to caffeoyl-CoA. Three isoforms of caffeoyl CoA *O*-methyltransferase (CCoAOMT1-3) methylate caffeoyl-CoA to give feruloyl-CoA, which is reduced to coniferaldehyde by a cinnamoyl-CoA reductase (CCR2). Two isoforms of CAld5H (CAld5H1 and CAld5H2) and one 5-hydroxyconiferaldehyde *O*-methyltransferase (AldOMT2) hydroxylate and methylate coniferaldehyde and coniferyl alcohol sequentially at the ring-5 position to give sinapaldehyde and sinapyl alcohol. The hydroxycinnamaldehydes are reduced to hydroxycinnamyl alcohols by two isoforms of cinnamyl alcohol dehydrogenase (CAD1 and CAD2). Cofactors are reduced NADPH, $NADP^+$, CoA, ATP, AMP, pyrophosphate (PP_i), *S*-adenosylmethionine (SAM), and *S*-adenosylhomocysteine (SAH).

key factors affecting plant resistance to pests and pathogens (Sarkanen and Ludwig, 1971) and the efficiency of lignin removal during conversion of secondary cell walls (biomass) into biofuels and materials (Sarkanen, 1976; Hu et al., 1999; Chiang, 2002; Ragauskas et al., 2006; Chen and Dixon, 2007; Novaes et al., 2010). Many transgenic plants or natural variants with modified lignin properties have been characterized, but our knowledge of the regulation of metabolic flux in monolignol biosynthesis is rudimentary and insufficient to predict the consequences of most transgenic perturbations and inadequate for the directed design of specific lignin properties. What is needed is a comprehensive understanding of the biosynthesis of monolignols

and regulation of the supply and ratios of these monomers, so predictive models can be developed to strategically optimize lignin content, composition, and structure as well as for plant growth and biomass utilization.

The estimation of the supply and ratio of monolignols for lignification requires comprehensive knowledge of the flux dynamics in the monolignol biosynthetic pathway. The phenylpropanoid/monolignol pathway consists of a large number of components (metabolites, enzymes, and cofactors) and reactions in a metabolic grid, where metabolic flux may be distributed in a matrix or in a single primary pathway. The complexity of biological pathways challenges any intuitive analysis of its regulation and metabolism (Schallau and Junker, 2010). Mathematical modeling is therefore appropriate to further understand these complex metabolic networks. A mathematical model of a biological pathway is a formal representation of our knowledge of the components of this pathway and the laws governing their functions and interactions. A kinetic model is assembled from a system of mechanistic nonlinear differential equations that defines dynamically the intracellular processes. Hence, a kinetic model is the most detailed and predictive mathematical description of a metabolic network and constitutes a significant branch in the growing field of systems biology (Schallau and Junker, 2010). Few such models have been presented in plant metabolism because of the difficulty in obtaining the comprehensive quantitative information required. The monolignol biosynthetic pathway is amenable to kinetic modeling because the major pathway enzymes and their isoforms have been identified and can be quantified (Shi et al., 2010; Shuford et al., 2012).

A few attempts have been made to quantitatively analyze and mathematically describe monolignol biosynthesis. Quantitative analysis of the efficiency of lignin biosynthesis was presented by Amthor (2003), who calculated the potential energy retention for 4-coumaroyl, coniferyl, and sinapyl alcohols. A mathematical model of monolignol biosynthesis in quaking aspen (*Populus tremuloides*) xylem based on published data (Osakabe et al., 1999; Harding et al., 2002; Li et al., 2003, 2005) using a static flux balance analysis and optimization-based nonlinear dynamic modeling was presented by Lee and Voit (2010). Such a model can only describe static fluxes and assessment of small perturbations. The static flux–based analyses were extended to include a Monte Carlo simulation of randomly parameterized kinetic models to suggest new metabolic control mechanisms for monolignol biosynthesis in alfalfa (*Medicago sativa*; Lee et al., 2011). These authors subsequently used a computational approach to analyze the hypothesis of metabolic channeling in the monolignol biosynthetic pathway of *Medicago* (Lee et al., 2012). The outputs of such models are largely hypothetical and are based on constraints that are not experimentally proven (Schallau and Junker, 2010). By contrast, comprehensive kinetic models that are based exclusively on differential equations with mass action kinetics are more likely to account for all regulatory and dynamic aspects of metabolic pathways and have substantive predictive value (Schallau and Junker, 2010). To build such a predictive kinetic metabolic-flux (PKMF) model of a biochemical pathway, one needs to know the stoichiometry of the pathway, including all enzymes, metabolites, and cofactors, plus the abundance of all isoforms of the enzymes and their reaction and inhibition kinetic parameters.

In this study, we constructed a PKMF model with a comprehensive experimental basis for the monolignol biosynthetic pathway in *P. trichocarpa* secondary differentiating xylem (SDX), a specialized tissue with abundant lignin biosynthesis. To build this PKMF model, we characterized the recombinant proteins for all pathway enzymes and their isoforms known from genome sequence (Shi et al., 2010), obtained or synthesized all pathway metabolites, and obtained an extensive set of reaction and inhibition kinetic parameters. We developed liquid chromatography–tandem mass spectrometry (LC-MS/MS) methods (Shuford et al., 2012) for absolute protein quantification of each of the multiple isoforms of the pathway enzymes expressed in SDX. The isoforms show different kinetic parameters and substrate specificities, information essential for predicting metabolic flux. Using these kinetic parameters and protein quantities, we derived a nonlinear ordinary differential equation (ODE) for each step of the pathway and integrated them using MATLAB. This PKMF model is based on Michaelis-Menten kinetics and obeys the law of mass conservation and was then used to evaluate the steady state flux distribution of the pathway and to predict regulatory mechanisms, lignin content, and composition.

RESULTS

The Production and Purification of Recombinant Proteins of All Known Monolignol Biosynthetic Pathway Enzymes in *P. trichocarpa*

The assembly of a PKMF model requires kinetic parameters of all pathway enzymes, which can be reliably estimated by in vitro analyses of purified recombinant proteins with known quantities. Functional recombinant proteins for all 21 *P. trichocarpa* monolignol enzymes were produced and purified (Figure 1), with the exception of a caffeoyl shikimic acid esterase (CSE). In *Arabidopsis thaliana*, a CSE that converts caffeoyl shikimic acid to caffeic acid has recently been identified (Vanholme et al., 2013). Two homologs of *CSE* are present in the genome of *P. trichocarpa* (Vanholme et al., 2013). In contrast with all known steps in monolignol biosynthesis (Figure 1), where we have demonstrated strong enzymatic activity in SDX protein extracts (Liu et al., 2012), SDX protein extracts of *P. trichocarpa* do not show CSE activity (Figure 2A). No factor in *P. trichocarpa* SDX protein extracts could inhibit the CSE activity to cause a complete absence of this activity (Figures 2A and 2B) because such extracts have no effect on the *Arabidopsis* stem CSE activity (Figures 2B). Therefore, CSE is not included in our model. Protein extracts from SDX of another woody dicot, *Eucalyptus grandis*, and the stems of two monocots, switchgrass (*Panicum virgatum*) and rice (*Oryza sativa*), also do not show CSE activity (Figure 2A). In *P. trichocarpa*, caffeoyl shikimic acid is converted to caffeoyl-CoA by two isoforms of hydroxycinnamoyl-CoA shikimate hydroxycinnamoyl transferase, HCT1 and HCT6.

To produce large amounts of proteins that can be readily purified, 6xHis-tagged or glutathione *S*-transferase (GST)–tagged soluble recombinant fusion proteins were produced in *Escherichia*

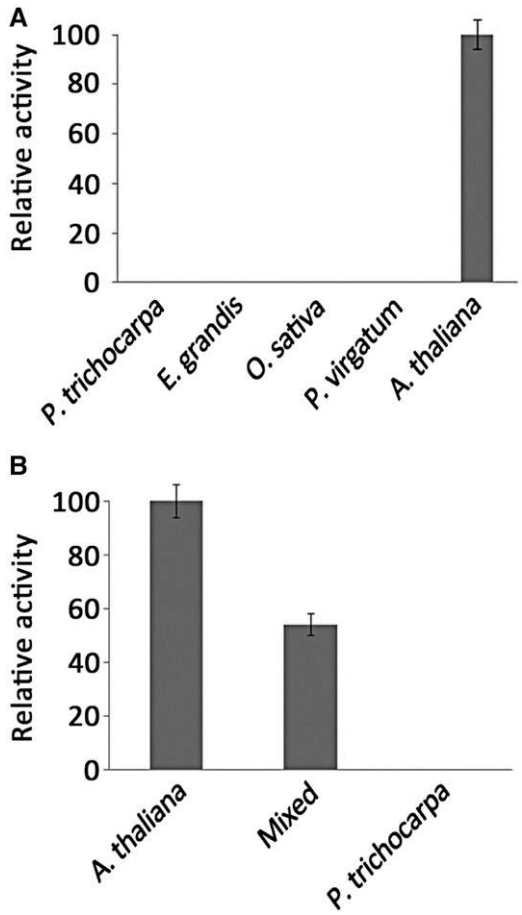

Figure 2. CSE Activity Is Detected in *Arabidopsis* but Not in *P. trichocarpa*, *E. grandis*, Rice, and Switchgrass.

(A) CSE activity in an extract of total proteins isolated from stems of *P. trichocarpa*, *E. grandis*, rice, switchgrass, and *Arabidopsis*.
(B) CSE activity in total proteins isolated from stems of *Arabidopsis*, 1:1 mixed proteins of *Arabidopsis* and *P. trichocarpa*, and *P. trichocarpa.* The error bars represent the SE of three technical replicates.

coli for five phenylalanine ammonia-lyase (*PAL*), two 4-coumaric acid:CoA ligase (*4CL*), two *HCTs*, one 5-hydroxyconiferaldehyde *O*-methyltransferase (*AldOMT*), three caffeoyl-CoA *O*-methyltransferase (*CCoAOMT*), one cinnamoyl-CoA reductase (*CCR*), and two cinnamyl alcohol dehydrogenase (*CAD*) genes. The membrane proteins, one coumaric acid 3-hydroxylase (C3H), two cinnamic acid 4-hydroxylases (C4Hs), and two coniferaldehyde 5-hydroxylases (CAld5Hs) were produced in *Saccharomyces cerevisiae* (Shuford et al., 2012; Wang et al., 2012; Chen et al., 2013; Supplemental Table 1). Six His amino acids were tagged to the C terminus and the fusion proteins were purified using a nickel chelating resin according to Chen et al. (2013). His tags generally have no significant effect on the structure and function of the native protein (Carson et al., 2007). C-terminal 6xHis fusions do not affect the substrate specificity and relative reaction rates of the two *P. trichocarpa* monolignol 4CLs (Chen et al., 2013). Soluble recombinant proteins with N-terminal GST tag fusions were purified using a glutathione sepharose chromatography resin (Shuford et al., 2012). The GST tags were subsequently cleaved using thrombin. *S. cerevisiae*–expressed recombinant membrane proteins were purified as microsomal fractions using ultracentrifugation (Chen et al., 2011; Shuford et al., 2012; Wang et al., 2012).

All purified soluble recombinant proteins were quantified using the Bradford method (Bradford, 1976). Previous studies of monolignol monooxygenase enzyme activities have been based on the weight of total crude microsomal proteins, as appropriate analytical tools were not available. However, such quantification is not adequate for deriving metabolic flux. We quantified the absolute abundance of the membrane proteins (one C3H, two C4Hs, and two CAld5Hs) expressed in yeast microsomes by our mass spectrometry–based method using protein-specific stable isotope-labeled (SIL) peptides as internal standards (Shuford et al., 2012; Wang et al., 2012).

Single Nucleotide Polymorphisms in the Monolignol Pathway Enzymes of *P. trichocarpa* Nisqually-1 Do Not Alter Their Enzyme Activities

Single nucleotide polymorphisms (SNPs) are ubiquitous in genomes of woody plants and can appear as frequently as one SNP in 16 base pairs in some species of *Eucalyptus* (Grattapaglia et al., 2011). Allelic variants may produce proteins that vary significantly in their kinetic properties and substrate preference and alter metabolic flux in their pathways. SNPs were identified (Supplemental Table 2) by deep sequencing of the *P. trichocarpa* SDX transcriptome. Thirty-three SNPs were found in the coding regions of the Nisqually-1 monolignol genes. Six were nonsynonymous, and they result in changes in amino acid sequences of 4CL3, CCoAOMT3, CCR2, CAld5H1, and CAld5H2. We previously evaluated the SNP variants of CAld5H1 and CAld5H2 and found that the SNPs have no effect on their activity (Wang et al., 2012). We produced purified recombinant proteins for the remaining nonsynonymous SNP variants, 4CL3, CCoAOMT3, and CCR2, and assayed their activity using 4-coumaric acid, caffeoyl-CoA, and feruloyl-CoA (3, 11, and 12 in Figure 1) as the respective substrates. These SNPs also have no effect on their enzymatic activities (Supplemental Figure 1).

Phosphoproteomic Studies Suggest That Monolignol Enzymes Are Not Phosphorylated

Phosphorylation is a common mode of posttranslational modification and has an important role in the regulation of metabolic flux in numerous plant metabolic pathways (Huber, 2007). Proteins may have very different reaction properties when they are phosphorylated (Huber, 2007). Such changes in reaction properties may have important regulatory roles in metabolic flux. To determine if any of the monolignol biosynthetic enzymes of *P. trichocarpa* are phosphoproteins, we evaluated the phosphoproteome of *P. trichocarpa* SDX using immobilized metal ion affinity chromatography–based phosphopeptide enrichment coupled with LC-MS/MS (Chen et al., 2013). A total of 147 phosphoproteins were identified. However, none of the phosphoproteins were the 21 monolignol biosynthetic pathway enzymes (Chen et al., 2013). An independent study using

a similar phosphopeptide enrichment/mass spectrometry strategy to analyze the phosphoproteome of dormant terminal buds of *P. simonii* × *P. nigra* identified 151 phosphoproteins (Liu et al., 2011). Again, none of these phosphoproteins were enzymes in the monolignol biosynthetic pathway.

Michaelis-Menten Kinetics of All Monolignol Pathway Enzymes

The construction of a PKMF model requires complete Michaelis-Menten and inhibition kinetic parameters for all enzymes in the pathway. We first determined the Michaelis-Menten kinetic parameter (K_m), the turnover number (k_{cat}), and the catalytic efficiency (k_{cat}/K_m) for all 21 enzymes (Figure 1) using optimized reaction conditions (Liu et al., 2012; Supplemental Table 3). The 24 monolignol biosynthetic pathway metabolites were obtained by chemical or biochemical synthesis or from commercial sources (Supplemental Methods 1). Single enzyme– and single substrate–based kinetic analyses were performed (Table 1). We previously reported the Michaelis-Menten kinetic parameters for PAL, C4H, C3H, 4CL, and CAld5H from *P. trichocarpa* (Chen et al., 2011; Wang et al., 2012; Shi et al., 2013). Here, we repeated the kinetic studies to determine the true catalytic turnover numbers for all hydroxylases (one C3H, two C4Hs, and two CAld5Hs), based on the mass spectrometry–based absolute protein quantity. In this study, we also determined the kinetic parameters of HCT, CCoAOMT, CCR, AldOMT, and CAD from *P. trichocarpa*.

PAL Catalytic Activity

The deamination of Phe to cinnamic acid in *P. trichocarpa* is catalyzed by five PALs (PAL1 to PAL5; Shi et al., 2010; V1 in Figure 1). These PAL family members have essentially identical catalytic activities, indicating functional redundancy (Table 1).

C4H Catalytic Activity

C4H1 and C4H2 are protein paralogs that share a 96.4% peptide sequence identity and mediate the conversion of cinnamic acid to 4-coumaric acid (V2 in Figure 1). These enzymes are kinetically distinct with different K_m and k_{cat} values (Table 1) and contribute differentially to the metabolic-flux converting cinnamic acid to 4-coumaric acid (Figure 1).

4CL Catalytic Activity

Two coenzyme-A ligases (4CL3 and 4CL5) are involved in *P. trichocarpa* SDX monolignol biosynthesis. Both 4CLs have broad substrate specificity, able to convert 4-coumaric, caffeic, ferulic, 5-hydroxyferulic, and sinapic acids to their hydroxycinnamyl-CoA derivatives (V7 to V11 in Figure 1, Table 1). These 4CLs have distinct reaction kinetic parameters (Chen et al., 2013). 4CL3 has the highest conversion rate for 4-coumaric acid, while CL5 can most effectively metabolize caffeic acid (Table 1).

C3H Catalytic Activity

A single C3H, C3H3, controls the 3-hydroxylation step in monolignol biosynthesis of *P. trichocarpa* (Shi et al., 2010; Figure 1). The 4-coumaric and 4-coumaroyl-shikimic acids are both 3-hydroxylated by C3H3, with 4-coumaroyl-shikimic acid having an ~40-fold higher catalytic efficiency than 4-coumaric acid. The low activity of 4-coumaric acid 3-hydroxylation may account for its difficult detection (Chen et al., 2011; Table 1). C3H3 has no 3-hydroxylation activity with 4-coumaroyl-CoA, 4-coumaraldehyde and 4-coumaryl alcohol, suggesting that 4-coumaric acid and 4-coumaroyl shikimic acid are the primary sources for G and S monolignol biosynthesis.

HCT Catalytic Activity

Two paralogous HCTs in *P. trichocarpa*, HCT1 and HCT6, mediate the reversible conversion of the hydroxycinnamyl-CoAs to their shikimate ester derivatives (V12 and V14 in Figure 1). Both HCT1 and HCT6 can convert 4-coumaroyl-CoA and caffeoyl-CoA into their shikimate ester derivatives efficiently (Table 1). However, the efficiency of converting 4-coumaroyl and caffeoyl shikimic acids to 4-coumaroyl-CoA and caffeoyl-CoA is very low. The pool of caffeoyl-CoA may need to be supplemented by alternative flux, such as 4CL-mediated CoA ligation of caffeic acid (Chen et al., 2013; V8 in Figure 1).

CCoAOMT Catalytic Activity

In *P. trichocarpa* , there are three xylem-specific CCoAOMTs (CCoAOMT1, CCoAOMT2, and CCoAOMT3; Shi et al., 2010). Caffeoyl-CoA and 5-hydroxyferuloyl-CoA are the two potential substrates of CCoAOMTs (Shi et al., 2010; V15 and 16 in Figure 1). However, 5-hydroxyferuloyl-CoA is not synthesized from feruloyl-CoA as the CAld5Hs have no such activity, and it is not synthesized from 5-hydroxyferulic acid as the 4CL activity is essentially abolished by the strong inhibitory effects of 4-coumaric, caffeic, and ferulic acids (Wang et al., 2012; Chen et al., 2013). We then focused on caffeoyl-CoA as the primary substrate to study the reaction kinetics of CCoAOMTs. All three CCoAOMTs can efficiently convert caffeoyl-CoA to feruloyl-CoA for monolignol biosynthesis in *P. trichocarpa*.

AldOMT Catalytic Activity

A single highly abundant and xylem-specific *AldOMT* transcript (*AldOMT2*) is found in the *P. trichocarpa* genome (Shi et al., 2010). AldOMT2 methylates the 3- or 5-hydroxyl groups of caffealdehyde, 5-hydroxyconiferaldehyde, caffeyl alcohol, and 5-hydroxyconiferyl alcohol (V4, V6, V22, V24, V30, and V32 in Figure 1) efficiently (Table 1). Caffeic and 5-hydroxyferulic acids are poor substrates for AldOMT2 (Table 1). Caffeoyl-CoA and 5-hydroxyferuloyl-CoA are not metabolized by AldOMT2.

CAld5H Catalytic Activity

CAld5H1 and CAld5H2 are functionally redundant proteins that mediate the 5-hydroxylation of coniferaldehyde and coniferyl alcohol for syringyl monolignol biosynthesis in *P. trichocarpa* (Wang et al., 2012; Table 1). Ferulic acid is a poor substrate for the CAld5Hs (Table 1).

Table 1. Michaelis-Menten Kinetic Parameters of the *P. trichocarpa* Monolignol Enzymes

Enzyme	Substrate	K_m (μM)	k_{cat} (min^{-1})	k_{cat}/K_m (μM^{-1} min^{-1})
PAL1	Phe	32.65 ± 0.10	88.05 ± 4.97	2.70 ± 0.15
PAL2	Phe	21.37 ± 0.44	63.93 ± 4.61	2.99 ± 0.16
PAL3	Phe	25.77 ± 2.71	93.49 ± 8.90	3.64 ± 0.04
PAL4	Phe	23.33 ± 1.04	71.68 ± 4.67	3.10 ± 0.32
PAL5	Phe	22.71 ± 0.13	75.78 ± 3.50	3.49 ± 0.17
C4H1	Cinnamic acid	7.06 ± 0.24	6.72 ± 0.04	0.95 ± 0.01
C4H2	Cinnamic acid	40.70 ± 1.48	21.41 ± 0.46	0.53 ± 0.08
4CL3	4-Coumaric acid	10.51 ± 2.84	44.48 ± 8.86	4.23 ± 1.44
	Caffeic acid	10.56 ± 2.44	17.07 ± 3.42	1.62 ± 1.44
	Ferulic acid	70.17 ± 4.37	50.33 ± 2.17	0.72 ± 0.05
	5-Hydroxyferulic acid	10.97 ± 1.25	3.08 ± 0.12	0.28 ± 0.03
4CL5	Caffeic acid	43.51 ± 5.43	43.69 ± 4.64	1.00 ± 0.16
	4-Coumaric acid	148.06 ± 14.04	106.83 ± 22.75	0.72 ± 0.17
	Ferulic acid	133.51 ± 7.02	68.41 ± 17.87	0.51 ± 0.14
	5-Hydroxyferulic acid	193.40 ± 21.54	37.34 ± 8.53	0.19 ± 0.05
	Sinapic acid	508.20 ± 37.26	20.79 ± 5.23	0.04 ± 0.01
C3H3	4-Coumaroyl shikimic acid	4.96 ± 0.10	57.79 ± 0.62	11.65 ± 0.27
	4-Coumaric acid	227.41 ± 15.62	67.92 ± 0.45	0.30 ± 0.02
HCT1	4-Coumaroyl-CoA	38.95 ± 4.96	138.35 ± 27.19	3.48 ± 0.28
	4-Coumaroyl shikimic acid	131.13 ± 9.21	5.23 ± 0.19	0.04 ± 0.0016
	Caffeoyl-CoA	23.06 ± 0.82	5.04 ± 0.13	0.22 ± 0.01
	Caffeoyl shikimic acid	572.07 ± 31.64	4.29 ± 0.18	0.0100 ± 0.0001
HCT6	4-Coumaroyl-CoA	24.91 ± 0.70	487.86 ± 36.36	19.53 ± 0.93
	4-Coumaroyl shikimic acid	91.38 ± 6.19	29.51 ± 1.27	0.33 ± 0.03
	Caffeoyl-CoA	103.81 ± 6.44	58.61 ± 6.73	0.56 ± 0.03
	Caffeoyl shikimic acid	415.60 ± 57.74	19.83 ± 0.22	0.05 ± 0.01
CCoAOMT1	Caffeoyl-CoA	29.78 ± 0.45	75.81 ± 6.14	2.55 ± 0.21
CCoAOMT2	Caffeoyl-CoA	19.10 ± 1.17	131.27 ± 10.38	6.87 ± 0.14
CCoAOMT3	Caffeoyl-CoA	23.07 ± 2.58	44.95 ± 3.26	1.95 ± 0.03
AldOMT2	Caffealdehyde	0.141 ± 0.014	4.518 ± 0.140	32.05 ± 3.36
	5-Hydroxyconiferaldehyde	0.23 ± 0.07	2.60 ± 0.38	11.19 ± 3.66
	Caffeyl alcohol	0.748 ± 0.039	6.173 ± 0.150	8.253 ± 0.472
	5-Hydroxyconiferyl alcohol	2.46 ± 0.83	15.38 ± 4.17	6.25 ± 2.75
	5-Hydroxyferulic acid	9.93 ± 1.22	5.55 ± 0.20	0.559 ± 0.072
	Caffeic acid	162.6 ± 8.2	2.995 ± 0.053	0.018422 ± 0.00098
CAld5H1	Coniferyl alcohol	0.0686 ± 0.0016	2.12 ± 0.03	30.90 ± 0.84
	Coniferaldehyde	0.0544 ± 0.0014	1.23 ± 0.02	22.61 ± 0.69
	Ferulic acid	19.30 ± 1.40	0.00077 ± 0.00001	0.000040 ± 0.000003
CAld5H2	Coniferyl alcohol	0.0526 ± 0.0044	1.72 ± 0.05	32.67 ± 2.90
	Coniferaldehyde	0.0453 ± 0.0004	1.008 ± 0.002	22.25 ± 0.20
	Ferulic acid	5.2 ± 0.2	0.001100 ± 0.000016	0.000211 ± 0.000009
CCR2	Feruloyl-CoA	44.89 ± 1.66	112.36 ± 6.29	2.51 ± 0.13
	4-Coumaroyl-CoA	259.81 ± 11.86	38.68 ± 1.90	0.15 ± 0.01
	Caffeoyl-CoA	581.07 ± 89.67	78.18 ± 13.94	0.14 ± 0.01
CAD1	Coniferaldehyde	0.68 ± 0.04	30.5 ± 1.6	45.5 ± 2.5
	4-Coumaraldehyde	2.97 ± 0.10	45.89 ± 4.99	15.50 ± 1.69
	Sinapaldehyde	2.4 ± 0.5	26.9 ± 2.6	11.4 ± 1.0
CAD2	Sinapaldehyde	35.4 ± 3.5	119 ± 11	3.37 ± 0.06
	Coniferaldehyde	70.0 ± 1.3	110 ± 4	1.58 ± 0.08

The values are means ± SE; $n = 3$.

CCR Catalytic Activity

In *P. trichocarpa*, a single CCR (CCR2) is abundantly and specifically expressed in the SDX (Shi et al., 2010); 4-coumaroyl-CoA, caffeoyl-CoA and feruloyl-CoA were tested as substrates for CoA reduction. CCR2 has a strong preference for the reduction of feruloyl-CoA into coniferaldehyde (V19 in Figure 1). The catalytic efficiency of CCR2 with 4-coumaryl-CoA (V17 in Figure 1) and caffeoyl-CoA (V18 in Figure 1) is significantly lower (Table 1).

CAD Catalytic Activity

In *P. trichocarpa*, two cinnamyl alcohol dehydrogenases (CAD1 and CAD2) mediate the reduction of the hydroxycinnamyl

aldehydes into monolignols (Shi et al., 2010; V25 to 29 in Figure 1). CAD1 and CAD2 are distinct in their kinetic properties for the production of monolignols (Table 1), where coniferaldehyde is the preferred substrate for CAD1; CAD2 has a higher catalytic efficiency for sinapaldehyde.

Inhibition Kinetics of the Monolignol Biosynthetic Enzymes

The Michaelis-Menten reaction kinetics of the *P. trichocarpa* monolignol biosynthetic pathway is the most complete for a single species (Table 1). The kinetic parameters describe exclusively the catalytic reaction of converting a substrate to its product. The reactions described are discrete and independent. However, in the monolignol biosynthetic pathway, intermediates may inhibit enzyme reactions upstream or downstream of specific metabolic steps (Kuroda et al., 1975; Jorrin and Dixon, 1990; Osakabe et al., 1999; Harding et al., 2002; Li et al., 2003, 2005; Wang et al., 2012; Chen et al., 2013; Shi et al., 2013). Such inhibitions play important roles in metabolic-flux distributions, which must be considered in a robust PKMF model. In a cellular environment where multiple metabolites are present (Chen et al., 2013), it is essential to define their roles as substrates and/or inhibitors for a more physiologically relevant kinetic metabolic-flux model. In this study, we report on the inhibition of five *P. trichocarpa* monolignol enzyme families, PAL (Shi et al., 2013), 4CL (Chen et al., 2011), CAld5H (Wang et al., 2012), AldOMT, and CAD (Table 2). The monolignol biosynthetic enzymes are inhibited by three modes of inhibition, competitive (K_{ic}), uncompetitive (K_{iu}), and substrate self-inhibition (K_{is}). Numerous substrate and inhibition combinations were tested for the remaining five monolignol enzyme families, but no significant inhibitions were found. A total of 89 inhibition parameters (K_{ic}, K_{iu}, and K_{is}) were determined based on 59 inhibition kinetic experiments (Table 2). These important regulatory effects are key factors in our PKMF model.

Inhibition of PAL Activity

We tested the inhibition reactions of all five PAL enzymes using cinnamic, 4-coumaric, caffeic and ferulic acids, and Tyr as the inhibitors. The PAL activity with Phe can be inhibited by cinnamic (2, Figure 1) and caffeic (4, Figure 1) acids for all five PALs (Sato et al., 1982; Jorrin and Dixon, 1990; Shi et al., 2013). No inhibition was found for 4-coumaric and ferulic acids or Tyr (Shi et al., 2013). All *P. trichocarpa* PALs are strongly inhibited by cinnamic and caffeic acids in predominantly competitive modes (K_{ic} values in Table 2 versus K_m values in Table 1). Cinnamic and caffeic acids are not only key intermediates in the pathway (Chen et al., 2011, 2013) but are also important regulators of PAL activity (Figure 3). These regulatory effects are important for determining the metabolic-flux in an integrated biosynthetic pathway.

Inhibition of 4CL Activity

All five hydroxycinnamic acid substrates (3 to 7 in Figure 1) of 4CL3 and 4CL5 were tested as inhibitors of the 4CL reaction. The 4CL3 activity with 4-coumaric, caffeic, and ferulic acids is inhibited through a pure competitive mode by all five hydroxycinnamic acids, while 4CL5 activity is regulated by three modes of inhibition, competitive, uncompetitive, and substrate self-inhibition (Chen et al., 2013; Figure 3, Table 2). Caffeic acid is the strongest inhibitor of both 4CL3 and 4CL5 (Table 2). Caffeic acid also causes substrate self-inhibition on 4CL5, but not on 4CL3 (Chen et al., 2013). The complex inhibition of 4CL activity suggests that this CoA ligation step is tightly regulated and that caffeic acid has a major regulatory role for monolignol biosynthesis in *P. trichocarpa*.

Inhibition of AldOMT Activity

Caffeic acid, 5-hydroxyferulic acid, caffealdehyde, 5-hydroxyconiferaldehyde, caffeyl alcohol, and 5-hydroxyconiferyl alcohols (5, 6, 17, 18, 22, and 23 in Figure 1) were tested as substrates and inhibitors of AldOMT2 activity. 5-Hydroxyconiferaldehyde and 5-hydroxyconiferyl alcohol are both strong inhibitors of AldOMT2 activity with any of the five substrates, with the K_{ic} and K_{iu} values (Table 2) much lower than the K_m (Table 1). Caffeic acid methylation by AldOMT2 is strongly inhibited by all five of the other compounds (Table 2). The methylation of hydroxycinnamyl aldehydes and alcohols is regulated by substrate self-inhibition, with the 5-hydroxylated moieties, such as 5-hydroxyconiferaldehyde and 5-hydroxyconiferyl alcohol, being more strongly inhibited than the 3-hydroxylated moieties, such as caffealdehyde and caffeyl alcohol (Figure 4, Table 2). The complex AldOMT2 inhibitory effects suggest a strong metabolic-flux control that ensures methylation occurs at the aldehyde and alcohol levels in monolignol biosynthesis. Understanding the effects of such complex regulation of metabolic flux is only possible by comprehensive mathematical modeling.

Inhibition of CAld5H Activity

Coniferaldehyde is a strong competitive inhibitor of ferulic acid 5-hydroxylation ($K_{ic} > K_m$) and a weak inhibitor of coniferyl alcohol 5-hydroxylation (Osakabe et al., 1999; Wang et al., 2012; Figure 5, Table 2). Coniferaldehyde and coniferyl alcohol are both viable substrates and regulators of 5-hydroxylation in monolignol biosynthesis (Osakabe et al., 1999; Wang et al., 2012).

Inhibition of CAD Activity

CAD1 is the predominant enzyme responsible for the reduction of cinnamaldehydes into monolignols. Coniferaldehyde and sinapaldehyde were tested as inhibitors of CAD1. We determined the extent and modes of inhibition of coniferaldehyde and sinapaldehyde on the CAD1-mediated biosynthesis of coniferyl and sinapyl alcohols (Figure 5). The enzymatic reduction of sinapaldehyde to sinapyl alcohol is strongly inhibited by coniferaldehyde following both competitive ($K_{ic} > K_m$; Tables 1 and 2) and uncompetitive ($K_{iu} > K_m$; Tables 1 and 2) modes. The inhibition of CAD1 mediated coniferaldehyde reduction by sinapaldehyde is weak ($K_m > K_{ic}$; Tables 1 and 2). Having obtained the reaction and inhibition kinetic parameters for the

Table 2. Inhibition Kinetic Parameters of the *P. trichocarpa* Monolignol Enzymes

Enzyme	Substrate	Inhibitor	K_{ic} (μM)	K_{iu} (μM)	K_{is} (μM)
PAL1	Phe	Cinnamic acid	13.44 ± 5.51		
	Phe	Caffeic acid	3.33 ± 2.73	13.44 ± 0.94	
PAL2	Phe	Cinnamic acid	8.72 ± 3.25	833.31 ± 2.82	
	Phe	Caffeic acid	5.17 ± 2.02	15.81 ± 1.57	
PAL3	Phe	Cinnamic acid	3.45 ± 0.64	49.42 ± 5.41	
	Phe	Caffeic acid	5.17 ± 2.02	15.81 ± 1.57	
PAL4	Phe	Cinnamic acid	9.02 ± 2.37		
	Phe	Caffeic acid	16.19 ± 5.23	15.67 ± 0.79	
PAL5	Phe	Cinnamic acid	5.50 ± 3.76		
	Phe	Caffeic acid	13.27 ± 1.9	42.45 ± 1.29	
4CL3	4-Coumaric acid	Caffeic acid	9.22 ± 2.68		
		Ferulic acid	55.05 ± 13.2		
		5-Hydroxyferulic acid	39.31 ± 3.95		
		Sinapic acid	78.11 ± 15.2		
	Caffeic acid	4-Coumaric acid	43.73 ± 1.09		
		Ferulic acid	59.36 ± 12.5		
		5-Hydroxyferulic acid	198.18 ± 10.03		
	Ferulic acid	4-Coumaric acid	13.12 ± 2.82		
		Caffeic acid	3.15 ± 0.26		
		5-Hydroxyferulic acid	7.63 ± 1.75		
		Sinapic acid	163.72 ± 14.4		
4CL5	4-Coumaric acid	Caffeic acid	7.06 ± 3.1	49.75 ± 7.80	
		Ferulic acid	335.54 ± 76.1	178.21 ± 60.70	
		5-Hydroxyferulic acid	48.8 ± 14.5	37.48 ± 5.94	
		Sinapic acid	631.72 ± 189.00	238.41 ± 44.70	
	Caffeic acid	4-Coumaric acid	122.7 ± 6.7	78.07 ± 10.83	
		Caffeic acid			55.97 ± 6.05
		Ferulic acid	518.93 ± 28.80	372.06 ± 73.26	
		5-Hydroxyferulic acid	45.36 ± 1.75	306.81 ± 40.59	
		Sinapic acid	2841.64 ± 101.25	157.21 ± 9.35	
	Ferulic acid	4-Coumaric acid	27.92 ± 3.70		
		Caffeic acid	18.47 ± 0.50	14.98 ± 0.67	
		5-Hydroxyferulic acid	185.78 ± 56.60	18.71 ± 4.62	
		Sinapic acid	384.85 ± 30.70	450.83 ± 4.10	
AldOMT2	Caffeic acid	Caffealdehyde	2.08 ± 0.46	7.57 ± 1.66	
		Caffeyl alcohol	1.63 ± 0.56	12.10 ± 4.20	
		5-Hydroxyferulic acid	38.62 ± 4.94	245.04 ± 31.38	
		5-Hydroxyconiferaldehyde	0.20 ± 0.03	2.70 ± 0.41	
		5-Hydroxyconiferyl alcohol	3.80 ± 0.44	23.23 ± 2.66	
	Caffealdehyde	Caffeic acid	174.68 ± 21.49		
		Caffealdehyde			14.8 ± 0.92
		5-Hydroxyferulic acid	19.79 ± 2.1		
		5-Hydroxyconiferaldehyde	0.55 ± 0.17	1.45 ± 0.31	
		5-Hydroxyconiferyl alcohol	0.7956 ± 0.1215		
	Caffeyl alcohol	Caffeyl alcohol			26.6 ± 1.43
		Caffealdehyde	5.65 ± 0.92	0.734 ± 0.055	
		5-Hydroxyconiferaldehyde	0.129 ± 0.011	0.542 ± 0.049	
		5-Hydroxyconiferyl alcohol		3.14 ± 0.68	
	5-Hydroxyconiferaldehyde	Caffealdehyde	0.287 ± 0.043		
		Caffeyl alcohol	2.50 ± 0.60	14.37 ± 1.865	
		5-Hydroxyconiferaldehyde			1.81 ± 0.14
		5-Hydroxyconiferyl alcohol	1.55 ± 0.46		
	5-Hydroxyconiferyl alcohol	5-Hydroxyconiferyl alcohol			2.28 ± 0.21
CAld5H1	Coniferyl alcohol	Coniferaldehyde	0.84 ± 0.03	1.7 ± 0.3	
	Ferulic acid	Coniferaldehyde	0.4 ± 0.03	1.5 ± 0.2	
CAld5H2	Coniferyl alcohol	Coniferaldehyde	18.8 ± 3.8		
	Ferulic acid	Coniferaldehyde	0.37 ± 0.07	1.00 ± 0.04	
CAD1	Sinapaldehyde	Coniferaldehyde	0.42 ± 0.39	1.92 ± 0.09	
	Coniferaldehyde	Sinapaldehyde	0.32 ± 0.19	3.02 ± 1.12	

The values are means ± SE; $n = 3$. Inhibitions that are absent or insignificant are left blank.

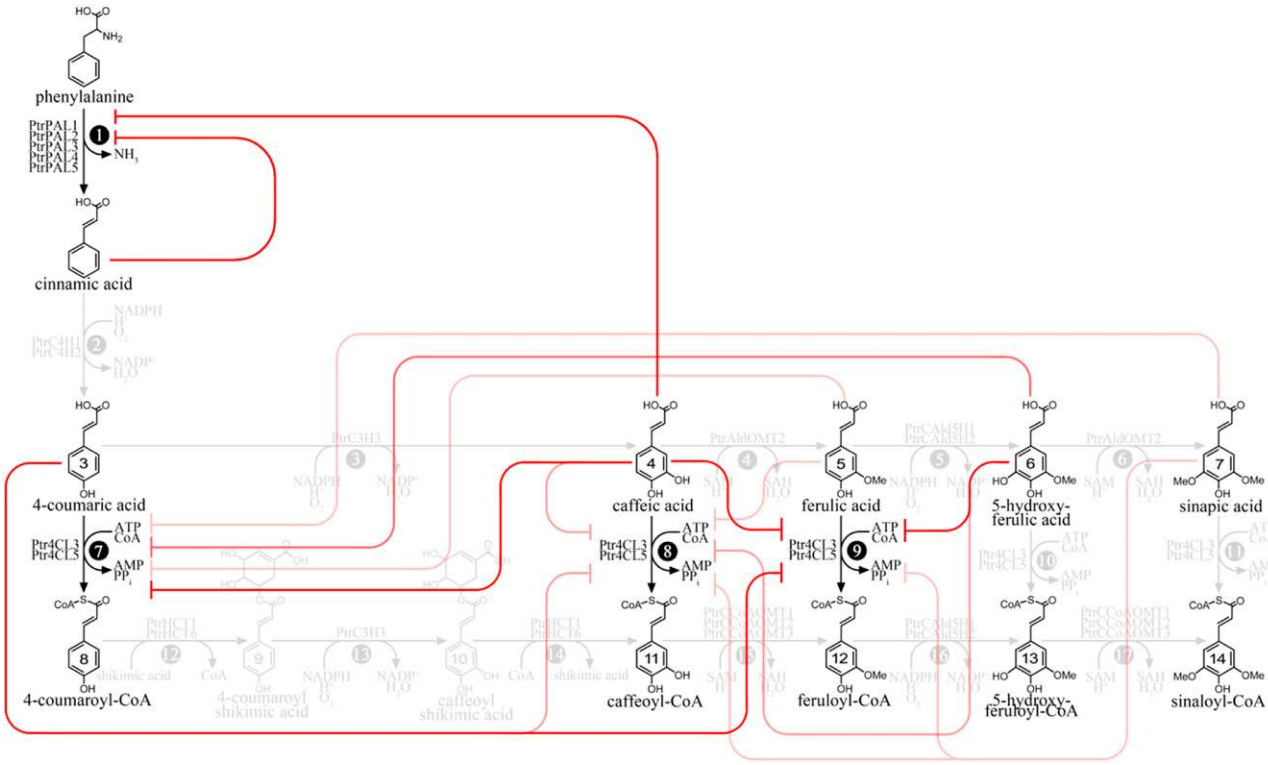

Figure 3. The Inhibition of *P. trichocarpa* PAL and 4CL Activity by Monolignol Pathway Intermediates.

The intensity of the red lines indicates the extent of inhibition.

monolignol enzymes in *P. trichocarpa*, we next quantified the absolute abundance of all 21 monolignol biosynthetic pathway enzymes in SDX.

Mass Spectrometry–Based Absolute Quantification of Monolignol Proteins in SDX of *P. trichocarpa*

We quantified the monolignol enzymes in SDX using protein cleavage coupled with isotope dilution mass spectrometry (PC-IDMS; Shuford et al., 2012). Protein-specific SIL peptides were used as internal standards for quantification of each enzyme. The respective target proteins were quantified based on the response ratio for the native SIL peptide pairs measured by nano-flow liquid chromatography coupled with selected reaction monitoring mass spectrometry. In this way, we obtained the absolute and comprehensive quantification of all 21 pathway enzymes in the SDX of *P. trichocarpa* (Supplemental Table 4). This quantification included all allelic variants of the monolignol pathway enzymes in *P. trichocarpa* Nisqually-1. The absolute quantitation of the monolignol enzymes in SDX of *P. trichocarpa*, together with the kinetic and inhibition parameters of the enzymes, is the foundation for generating the PKMF model through a system of ODEs to mathematically represent metabolic flux in monolignol biosynthesis. PAL4 and PAL5 were not quantified separately because they cannot be differentiated by PC-IDMS (Shuford et al., 2012).

PKMF Model Formulation

To predict the steady state flux distribution and to understand how individual enzyme families in the monolignol biosynthetic pathway regulate lignin content, composition, and flux distribution, we used the complete set of experimentally derived kinetic and absolute protein quantity data to assemble a mathematical model, the PKMF model. To construct this model, we first defined a static model of the monolignol biosynthetic pathway in *P. trichocarpa*. Then, ODEs were formulated, and the steady state flux distribution was solved using MATLAB. The MATLAB codes with detailed instructions on how to download and setup the PKMF model in MATLAB and how to use these codes to predict metabolic flux for the wild type and specific perturbations can be found at http://ligninsystems.org/matlab_pkmf.

Static Model of the Monolignol Biosynthetic Pathway in P. trichocarpa

Prior to modeling metabolic flux, we must first define the boundaries and components of the monolignol biosynthetic pathway in *P. trichocarpa* as a static model (Figure 1). This static model comprises 21 enzymes, 24 metabolites, and 35 metabolic fluxes. The input of this static model is the influx of Phe (V0 in Figure 1), and the outputs are the efflux of the three monolignols: 4-coumaryl alcohol (V33 in Figure 1), coniferyl alcohol (V34 in Figure 1), and sinapyl alcohol (V35 in Figure 1) for polymerization.

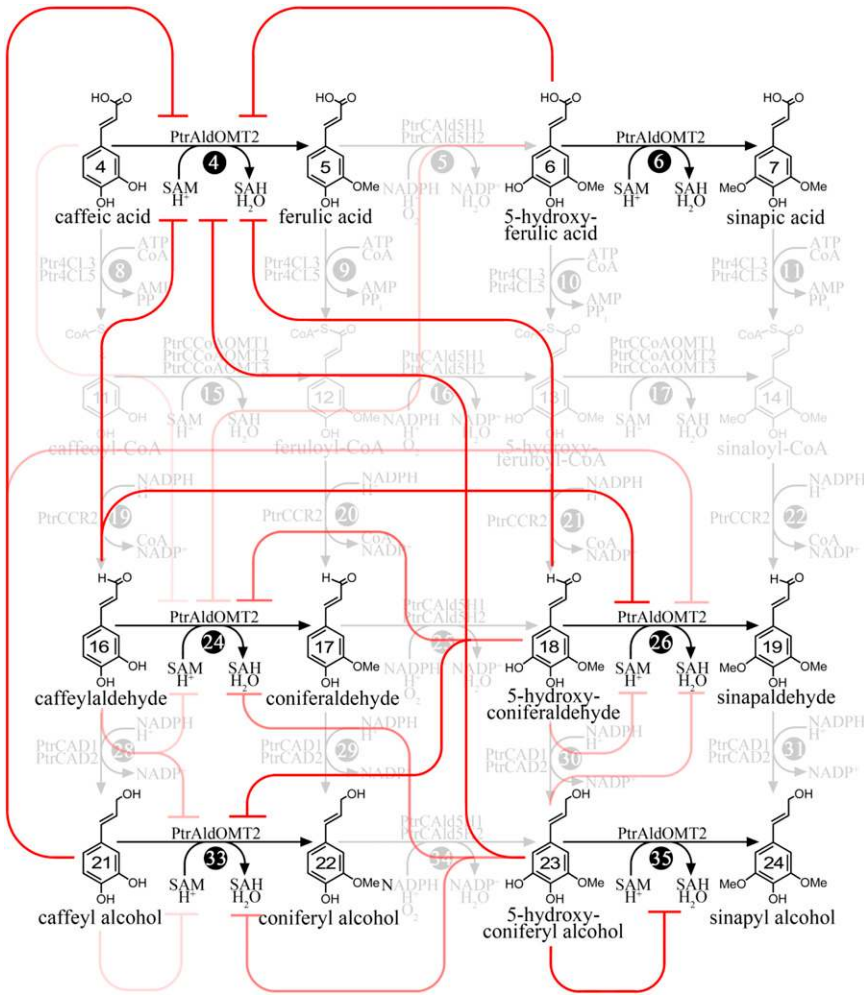

Figure 4. Inhibition of the AldOMT2-Catalyzed Methylation Step in Monolignol Biosynthesis of *P. trichocarpa*.

The intensity of the red lines indicates the extent of inhibition. The methylation of caffeic acid is strongly inhibited both competitively and uncompetitively by the five other substrates of AldOMT2. The methylation of caffealdehyde is strongly inhibited by 5-hydroxyconiferaldehyde and 5-hydroxyconiferyl alcohol and weakly inhibited by caffeic acid and 5-hydroxyferulic acid. Caffeyl alcohol methylation is strongly inhibited by caffealdehyde and 5-hydroxyconiferaldehyde and weakly inhibited by 5-hydroxyconiferyl alcohol. 5-Hydroxyconiferaldehyde is strongly inhibited competitively by caffealdehyde and weakly inhibited by caffeyl alcohol and 5-hydroxyconiferyl alcohol.

We next composed a set of ODEs to mathematically describe this static model.

Formulating a Set of ODEs and Integrating Reaction and Inhibition Kinetic Parameters and Absolute Protein Quantity

A metabolic pathway can be represented mathematically by assuming mass conservation between the production and consumption of the metabolites. A differential equation can then be defined for each metabolite where changes in the concentration of the metabolite S_i are dependent upon the rate of its production (V_{in}) and the rate of its consumption (V_{out}) (Equation 1). At steady state, the difference between these rates is zero.

$$\frac{dS_i}{dt} = V_{in} - V_{out} \quad (1)$$

Using the static model described earlier, we assembled a set of ODEs to describe changes in the concentrations of each pathway metabolite as a function of time (Table 3). The reaction and inhibition kinetic parameters derived using recombinant proteins and the absolute proteins abundance in SDX obtained using mass spectrometry were incorporated into the ODEs. These ODEs are the building blocks for PKMF modeling.

Simulation Using ODEs in MATLAB to Generate a PKMF Model

The ODEs were numerically integrated into MATLAB R2011a using ODE solver (ODE23tb; Shampine, 1994) to simulate pathway metabolic flux. The steady state pathway flux pattern is obtained as a function of the flux input, the reaction and inhibition kinetic parameters, and the absolute abundance of the

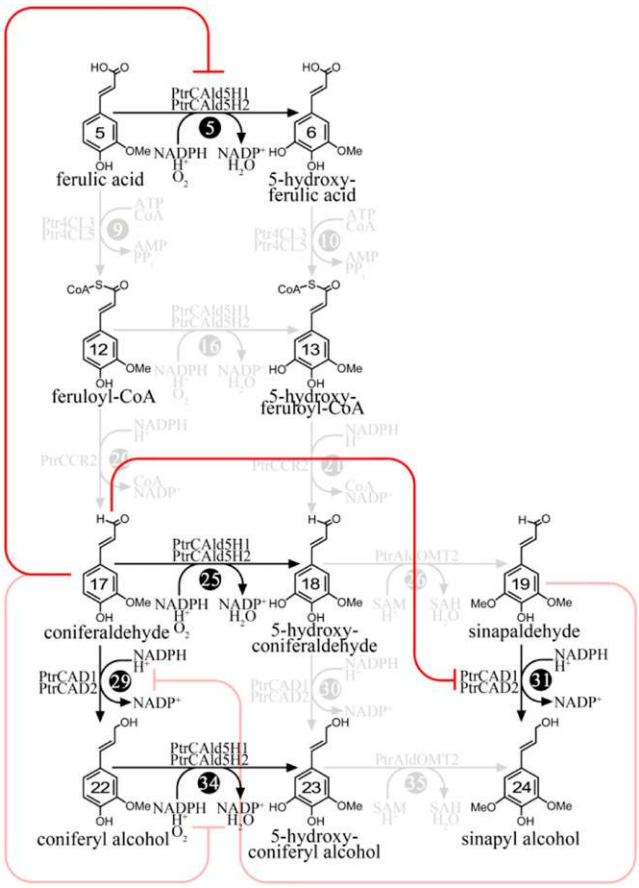

Figure 5. The Inhibition of CAD and CAld5H Activity by Monolignol Pathway Intermediates.

The intensity of the red lines indicates the extent of inhibition.

enzymes in SDX. As the PKMF model obeys the laws of mass conservation, the input flux V0 is equal to the sum of the exit fluxes V33, V34, and V35, and at steady state, these fluxes are constant. The exit fluxes V33, V34, and V35 denote the rates at which 4-coumaryl, coniferyl, and sinapyl alcohols are transported and polymerized to H, G, and S subunits in lignin, respectively. Therefore, the ratio of V35 and V34 predicts lignin S/G ratio, and the sum of V33, V34, and V35 predicts total lignin content. To define the input flux (V0 in Figure 1) for monolignol biosynthesis in wild-type *P. trichocarpa*, a particle swarm optimization algorithm (Kennedy and Eberhart, 1995) was used to solve for V0 when the S/G ratio (V35/V34) in polymeric lignin is 2.09, a true quantity based on two dimensional–nuclear magnetic resonance analysis of isolated lignin from stem wood of *P. trichocarpa* (Lu et al., 2013).

Particle swarm optimization is a stochastic optimization method effective at solving objective functions with multiple maxima and minima. The specific properties of the enzymes and their quantities require a specific influx (V0) of 0.904 $\mu M \cdot min^{-1}$ to make a lignin S/G ratio of 2.09. Implementing this V0 into the PKMF model and solving for steady state produces a metabolic-flux distribution for the wild type (Figure 8B). A principle metabolic flux leads to the biosynthesis of G and S monolignols, with an S monolignol–specific metabolic-flux branching from the principle flux at coniferaldehyde. A small amount of metabolic-flux stems from the principal flux at 4-coumaroyl-CoA (8 in Figure 1) for the biosynthesis of H monolignol. This metabolic-flux distribution is consistent with our knowledge of H, G, and S monolignol biosynthesis (Wang et al., 2012). We next validated the PKMF model using experimental data obtained from transgenic *P. trichocarpa*.

Validation of the PKMF Model Using Experimental Data Measured for Transgenic *P. trichocarpa*

The PKMF model can predict how changes in the protein abundance of monolignol pathway enzymes affect lignin content and composition. To validate the predictive power of this PKMF model, we compared the model predictions to experimental data obtained from transgenic *P. trichocarpa*.

We generated a large series of transgenic *P. trichocarpa* lines downregulated in a xylem-specific manner, for one or more members of the PAL family (Supplemental Methods 2, Supplemental Figure 2, and Supplemental Table 5). This produced transgenic lines with a wide spectrum of PAL protein abundance in the SDX. We selected seven transgenic lines and three wild types where total PAL protein abundance varied from 406 to 4 nM and lignin content from 21 to 12% of total dry weight of wood (Figure 6A). Using the PKMF model, we predict how changes in the protein abundance of the five PALs affect lignin content (Figure 6B). The PKMF model prediction fits the experimental data, both showing that the lignin content is not affected until the total PAL protein abundance is dramatically reduced, consistent with earlier studies (Sewalt et al., 1997; Song and Wang, 2011). Having validated the PKMF model using PAL transgenics, we next used the model to investigate the predicted effects of the abundance of the remaining monolignol enzyme families on lignin content and composition.

How Lignin Content and S/G Ratio Are Affected by Protein Abundance of Individual Enzyme Families

To investigate how the protein abundance of the individual pathway enzyme families in the PKMF model affect lignin content and S/G ratio, we systematically varied the protein abundance of the individual monolignol enzyme families from 100 to 0% of the wild type in the PKMF model and predicted the consequent lignin content and S/G ratio (Figure 7). A reduction in C4H shows no effect on lignin until the protein abundance is 12% of the wild type and results in low lignin and a high S/G ratio (Figures 7B and 7L). The abundance of CAld5H proteins does not affect total lignin content but is linearly proportional to the lignin S/G ratio (Figures 7I and 7S). Reduction in C3H shows no effect until protein concentration is below 24% of the wild type and results in reduced lignin and increases in S/G ratio (Figures 7C and 7M). The abundance of AldOMT must be below 10% of the wild type before the S/G ratio and lignin content is reduced (Figures 7H and 7R). Reduction of HCT to 50% of the wild type results in reduced quantity of lignin and an increase in S/G ratio. However, when the abundance of HCT falls below

Table 3. The ODEs for the 24 Lignin Precursors

Metabolites	Mass Balance Equations
Phe	$\frac{dS_1}{dt} = V_0 - V_1$
Cinnamic acid	$\frac{dS_2}{dt} = V_1 - V_2$
4-Coumaric acid	$\frac{dS_3}{dt} = V_2 - V_3 - V_7$
Caffeic acid	$\frac{dS_4}{dt} = V_3 - V_4 - V_8$
Ferulic acid	$\frac{dS_5}{dt} = V_4 - V_5 - V_9$
5-Hydroxyferulic acid	$\frac{dS_6}{dt} = V_5 - V_6 - V_{10}$
Sinapic acid	$\frac{dS_7}{dt} = V_6 - V_{11}$
4-Coumaryl-CoA	$\frac{dS_8}{dt} = V_7 - V_{12} - V_{17}$
4-Coumaryl shikimic acid	$\frac{dS_9}{dt} = V_{12} - V_{13}$
Caffeoyl shikimic acid	$\frac{dS_{10}}{dt} = V_{13} - V_{14}$
Caffeoyl-CoA	$\frac{dS_{11}}{dt} = V_8 + V_{14} - V_{15} - V_{18}$
Feruloyl CoA	$\frac{dS_{12}}{dt} = V_9 + V_{15} - V_{19}$
5-Hydroxyferuloyl-CoA	$\frac{dS_{13}}{dt} = V_{10} - V_{16} - V_{20}$
Sinapoyl-CoA	$\frac{dS_{14}}{dt} = V_{11} + V_{16} - V_{21}$
4-Coumaraldehyde	$\frac{dS_{15}}{dt} = V_{17} - V_{25}$
Caffealdehyde	$\frac{dS_{16}}{dt} = V_{18} - V_{22} - V_{26}$
Coniferaldehyde	$\frac{dS_{17}}{dt} = V_{19} + V_{22} - V_{23} - V_{27}$
5-Hydroxyconiferaldehyde	$\frac{dS_{18}}{dt} = V_{20} + V_{23} - V_{24} - V_{28}$
Sinapaldehyde	$\frac{dS_{19}}{dt} = V_{21} + V_{24} - V_{29}$
4-Coumaryl alcohol	$\frac{dS_{20}}{dt} = V_{25} - V_{33}$
Caffeyl alcohol	$\frac{dS_{21}}{dt} = V_{26} - V_{30}$
Coniferyl alcohol	$\frac{dS_{22}}{dt} = V_{27} + V_{30} - V_{31} - V_{34}$
5-Hydroxyconiferyl alcohol	$\frac{dS_{23}}{dt} = V_{28} + V_{31} - V_{32}$
Sinapyl alcohol	$\frac{dS_{24}}{dt} = V_{29} + V_{32} - V_{35}$

S_n refers to the compound numbers in Figure 1; V_n refers to the fluxes in Figure 1.

10% of the wild type, lignin content begins to increase until it approximates the lignin content of the wild type (Figures 7D and 7N). Reduction in CCR to 10% of the wild type results in a reduction in lignin and an increase in S/G ratio (Figures 7F and 7P). Reduction in CAD to 50% of the wild type results in a reduction in lignin content and a reduction in the S/G ratio (Figures 7J and 7T).

These predictions show that, a reduction in flux, even for early steps in the pathway can dramatically affect the S/G ratio. This result appears paradoxical. However, it is the combined effects of the kinetic properties of the enzymes late in the pathway and the level of flux that cause the change in S/G ratio (see Changes in the Abundance of Early Pathway Proteins Affect Lignin S/G Ratio in Discussion).

How Pathway Metabolic-Flux Distribution Is Affected by Protein Abundance of Individual Enzyme Families

The previous results focused on the prediction of lignin content and composition. Here, we show how our PKMF model predicts metabolic-flux distribution, which provides knowledge of the regulatory mechanisms affecting lignin content and composition. To do this, we reduced the abundance of the individual monolignol enzyme families to 1% of the wild type, a protein level where all enzyme families affect lignin, and predicted the consequent pathway flux distribution. The PKMF model indicates that the individual monolignol enzyme families are unique such that different levels of protein reductions are required to affect lignin content and S/G ratio (Figure 8). Two types of responses in the pathway flux distribution are observed when the monolignol enzyme families are reduced. The reduction in protein abundance either activates an alternative pathway for monolignol biosynthesis, or it creates a block where the majority of the metabolic flux is not used for monolignol biosynthesis.

For the 4CL, HCT, and CCoAOMT enzyme families, a reduction in the protein abundance results in an activation of alternative pathways to direct metabolic flux for monolignol biosynthesis. When the concentration of 4CL proteins is reduced, the principle metabolic flux through the 3-hydroxylation and subsequent 3-methylation steps shift from the pathway involving phenolic shikimic acids and CoA thioesters (Figure 8B; V12 to V15 in Figure 1) to hydroxycinnamic acids (Figure 8E; V3 and V4 in Figure 1). The CoA ligation step then proceeds through the metabolism of ferulic acid (Figure 8E) instead of through 4-coumaric and caffeic acids (Figure 8B). These results are consistent with our previous finding that the 3-hydroxylation step is mediated through both the shikimic acid esters and directly to caffeic acid (Chen et al., 2011). When the HCT abundance is reduced (Figure 8J), the principal metabolic flux is directed to the biosynthesis of H monolignol at V17 (Figure 1), instead to the biosynthesis of G and S monolignols. This prediction is consistent with the HCT-downregulated transgenic plants (Hoffmann et al., 2004; Shadle et al., 2007). When CCoAOMT abundance is reduced (Figure 8H), the principal pathway between caffeoyl-CoA and coniferaldehyde changes from feruloyl-CoA as in the wild type (Figure 8B; 11 to 12 to 17 in Figure 1) to caffealdehyde (Figure 8H; 11 to 16 to 17 in Figure 1). Lee et al. (2011) also suggested that the 3-methoxylation of caffealdehyde may be an alternative pathway for monolignol biosynthesis.

For PAL, C4H, C3H, AldOMT, CCR, and CAD enzyme families, a reduction in the abundance of proteins does not activate alternative pathways. Instead, it reduces the principal metabolic flux for monolignol biosynthesis (Figures 8C, 8D, 8F, 8G, 8I, 8K, and 8L). These predicted effects on lignin are now compared with published literature data on transgenic plants perturbed in the transcript levels of the monolignol biosynthetic pathway genes.

The PKMF Model Strengthens Previous Knowledge and Predicts Regulatory Mechanisms in Monolignol Biosynthesis

A strong reduction in the abundance of PAL proteins is required to impact lignin deposition (Figure 7A), suggesting that PAL activity is present in excess for monolignol biosynthesis. This prediction is consistent with PAL transgenic tobacco (*Nicotiana tabacum*; Bate et al., 1994). Severe reduction in PAL abundance leads to decreased levels of lignin and increased S/G ratio, also consistent with previous transgenic studies (Sewalt et al., 1997; Song and Wang, 2011). The PKMF model predicts that a severe reduction in the C4H protein abundance results in a reduction in lignin content. The lignin content of C4H transgenic plants of tobacco (Sewalt et al., 1997), alfalfa (Reddy et al., 2005), tomato (*Solanum lycopersicum*; Millar et al., 2007), *Arabidopsis* (Schilmiller et al., 2009), and hybrid aspen (*Populus tremula* × *tremuloides*; Bjurhager et al., 2010) is consistent with our predictions. The S/G ratios of C4H transgenic plants are inconsistent.

A

Lines	[PAL1] (nM)	[PAL2] (nM)	[PAL3] (nM)	[PAL4/5] (nM)	[total PALs] (nM)	Lignin %
WT1	39.43	111.3	32.77	223	406.5	19.8
WT2	35.97	116.4	20.59	163	335.96	21.3
WT3	31.91	107.6	24.39	153.8	317.7	20.3
T1	24.33	86.37	0	154.1	264.8	21.2
T2	5.486	73.74	14.88	104.7	198.806	21.2
T3	32.37	20.47	17.37	18.12	88.33	21.7
T4	23.83	17.36	14.83	13.8	69.82	20.9
T5	5.881	0	2.681	1.933	10.495	14.6
T6	2.262	0	1.586	1.624	5.472	12.3
T7	3.799	0	0	0	3.799	13.7

B

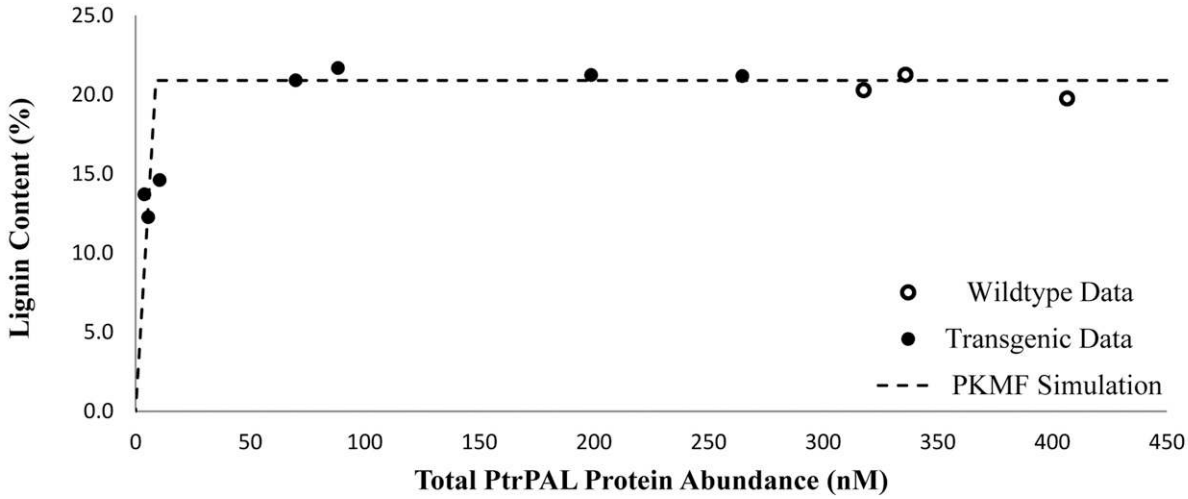

Figure 6. Validation of the PKMF Model Using Transgenic *P. trichocarpa* with Xylem-Specific PAL Downregulation.

(A) The protein levels of the five PAL and lignin content for the three wild types and seven transgenic lines (T). The shading for total PALs graphically indicates the protein abundance given by the respective numbers.

(B) Coincidence between the PKMF model simulation (dashed line) and experimental data obtained from transgenic (solid dot) and wild-type (open circle) *P. trichocarpa*.

C4H-downregulated transgenic tomato and an *Arabidopsis* mutant showed an increase in S/G ratio, consistent with our model prediction. However, transgenic tobacco and alfalfa showed a decrease in S/G ratio, and hybrid aspen showed no change in S/G ratio. These inconsistencies may be due to species-specific regulation of the pathway.

When 4CL protein abundance is reduced, the PKMF model predicts a reduction in lignin content and an increase in S/G ratio. Transgenic tobacco (Kajita et al., 1996), *Arabidopsis* (Lee et al., 1997), aspen (Hu et al., 1999), radiata pine (*Pinus radiata*; Wagner et al., 2009), hybrid poplar (*Populus tremula* × *Populus alba*; Kitin et al., 2010; Voelker et al., 2010), and switchgrass (Xu et al., 2011), downregulated in 4CL, all showed a reduction in lignin content, consistent with model predictions. In addition, the model predicts that the principal metabolic-flux shifts from 4-coumaroyl-CoA to feruloyl-CoA (Figure 8B) and then is diverted to 4-coumaric acid and to ferulic acid (Figure 8E). This shift provides an explanation for the accumulation of soluble and wall-bound hydroxycinnamic acids, such as 4-coumaric and ferulic acids in transgenic plants with severe 4CL downregulation in tobacco and aspen (Kajita et al., 1996; Hu et al., 1999). Also, as predicted by the PKMF model, tobacco, *Arabidopsis*, and switchgrass exhibited an increase in the S/G ratio when 4CL is reduced. However, the S/G ratio of transgenic hybrid poplar decreased when 4CL expression was downregulated. This difference suggests that the S/G ratio in hybrid poplar is regulated by novel mechanisms in addition to the abundance and properties of the monolignol pathway enzymes.

When the protein abundance of C3H3 is reduced, the PKMF model predicts a reduction in lignin content, an increase in H subunits, and an increase in S/G ratio. These predictions are consistent with transgenic alfalfa (Reddy et al., 2005) and hybrid poplar (Coleman et al., 2008) downregulated in C3H. HCT is involved in two reactions in the monolignol pathway: the conversion of 4-coumaroyl-CoA to 4-coumaroyl shikimic acid (V12 in Figure 1) and the conversion of caffeoyl shikimic acid to caffeoyl-CoA (V14 in Figure 1). An initial reduction in lignin content is observed when HCT abundance is between 50 and 10% of the wild type. This reduced lignin content results from metabolic flux being blocked at the conversion of caffeoyl shikimic acid to caffeoyl-CoA (V14 in Figure 1), as the catalytic efficiency of this reaction is much lower than the conversion of 4-coumaroyl-CoA to 4-coumaroyl-shikimic acid (V12 in Figure 1).

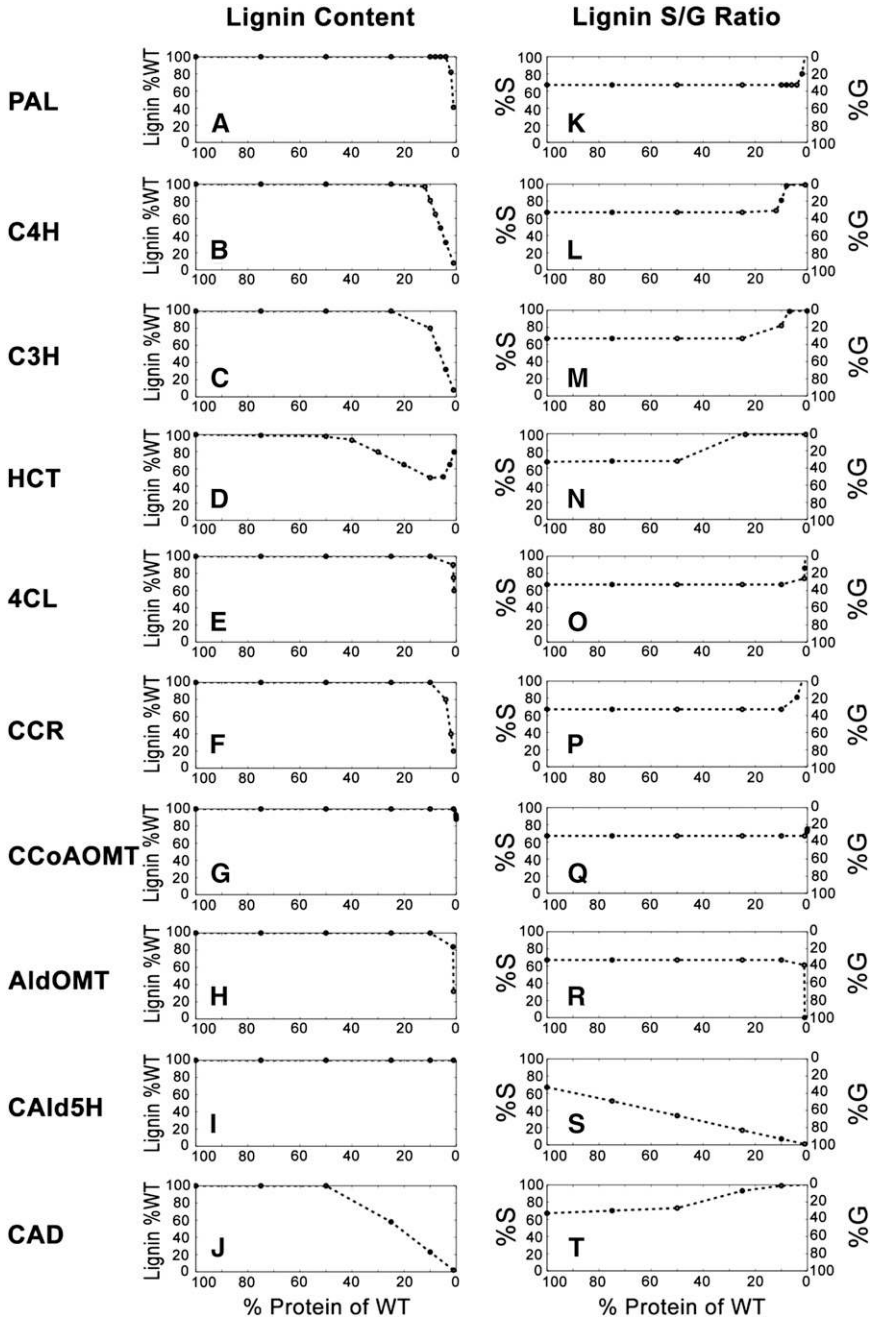

Figure 7. PKMF Model Simulation of the Effects of Downregulating Individual Monolignol Enzyme Families.

Downregulation from 100 to 0% of the wild type on lignin content **(A)** to **(J)** and lignin S/G ratio **(K)** to **(T)**.

However, when HCT abundance is reduced below 10% of the wild type, 4-coumaroyl-CoA is preferentially converted to 4-coumaraldehyde (V17 in Figure 1) by CCR2 for H lignin biosynthesis instead of to 4-coumaroyl shikimic acid by the HCTs. As a result of this change in metabolic-flux distribution, lignin content is increased to approximately the level of the wild type but consists of almost entirely of H subunits. These PKMF model predictions are consistent with transgenic alfalfa (Shadle et al., 2007), tobacco, and *Arabidopsis* (Hoffmann et al., 2004) downregulated in HCT.

When CCoAOMT abundance is reduced, the PKMF model predicts that lignin content is reduced and the S/G ratio is increased. These predictions are consistent with transgenic tobacco (Zhong et al., 1998), hybrid poplar (Meyermans et al., 2000; Zhong et al., 2000), alfalfa (Guo et al., 2001; Marita et al., 2003), and *Arabidopsis* (Do et al., 2007) downregulated in

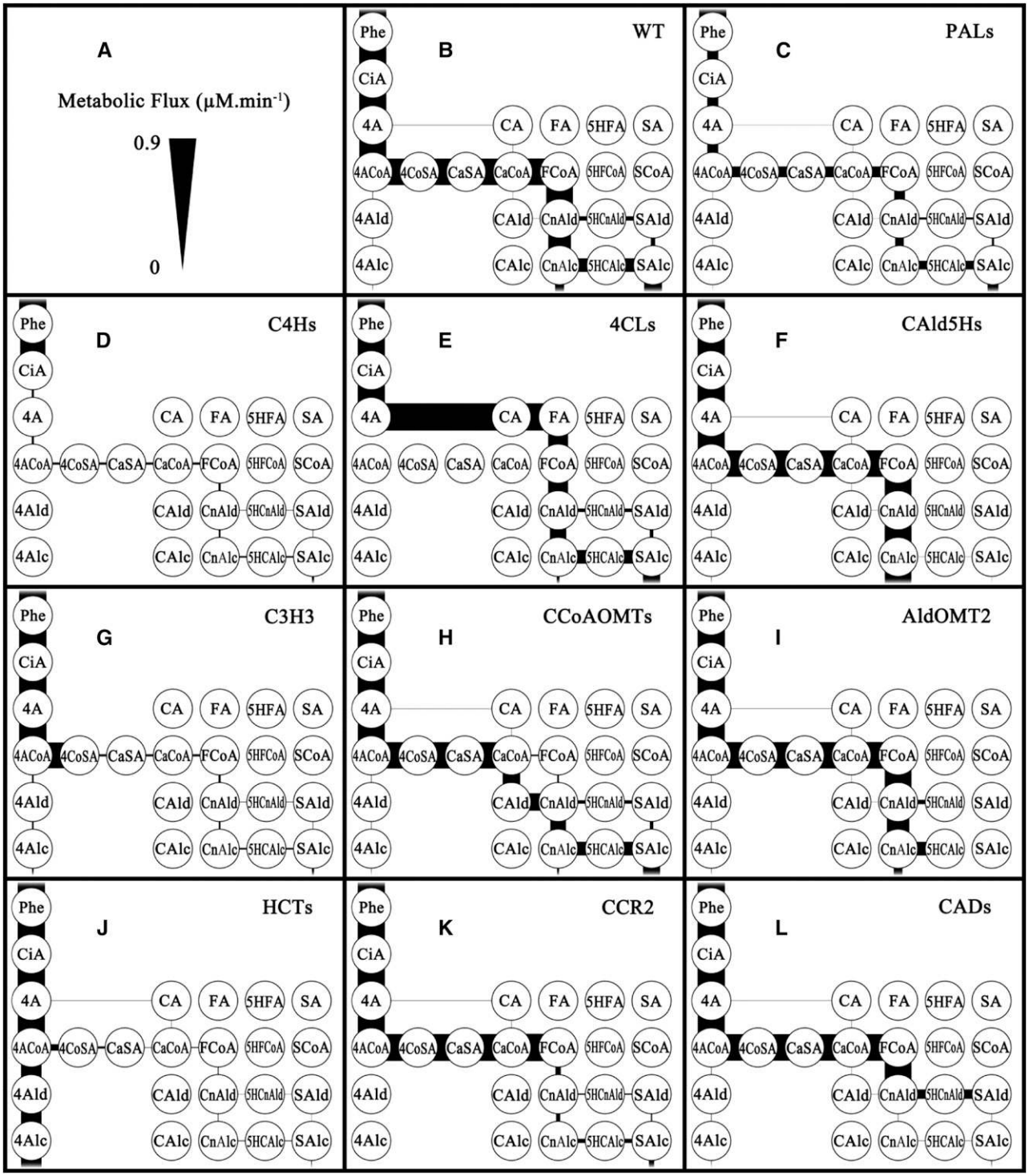

Figure 8. PKMF Model Simulation of the Effects of Downregulating Individual Monolignol Enzyme Families on Pathway Metabolic-Flux Distribution.

The thickness of the lines represents the amount of metabolic flux through that portion of the pathway. Steady state metabolic-flux distributions of the monolignol biosynthetic pathway for wild-type *P. trichocarpa* **(B)** and *P. trichocarpa* with downregulation of specific monolignol enzyme family protein abundance to 1% of the wild type (**[C]** to **[L]**). CiA, cinnamic acid; 4A, 4-coumaric acid; CA, caffeic acid; FA, ferulic acid; 5HFA, 5-hydroxyferulic acid; SA, sinapic acid; 4ACoA, 4-coumaroyl-CoA; 4CoSA, 4-coumaroyl shikimic acid; CaSA, caffeoyl shikimic acid; CaCoA, caffeoyl-CoA; FCoA, feruloyl-CoA; 5HFCoA, 5-hydroxyferuloyl-CoA; SCoA, sinapoyl-CoA; 4Ald, 4-coumaraldehyde; CAld, caffealdehyde; CnAld, coniferaldehyde; 5HCnAld, 5-hydroxyconiferaldehyde; SAld, sinapaldehyde; 4Alc, 4-coumaryl alcohol; CnAlc, coniferyl alcohol; 5HCnAlc, 5-hydroxyconiferyl alcohol; SAlc, sinapyl alcohol.

CCoAOMT expression. Downregulation of CCoAOMT in radiata pine (Wagner et al., 2011) showed a reduction in lignin content as a result of reduced G subunits, also consistent with the PKMF predictions.

In the near absence of the AldOMT2 protein, the PKMF model predicts that the metabolic flux for G monolignol subunit synthesis remains unaffected, whereas the metabolic flux for the synthesis of S monolignol subunits is abolished at 5-hydroxyconiferaldehyde and 5-hydroxyconiferyl alcohol (Figure 8I). These 5-hydroxyguaiacyl moieties could then be incorporated into lignin. These predictions are consistent with results from transgenic tobacco, quaking aspen, hybrid poplar, alfalfa, maize (*Zea mays*), and white lead tree (*Leucaena leucocephala*; Dwivedi et al., 1994; Tsai et al., 1998; Meyermans et al., 2000; Guo et al., 2001; Piquemal et al., 2002; Rastogi and Dwivedi, 2006) reduced in AldOMT activity. Reduction in AldOMT generally results in a mild decrease in lignin content, severe reduction in syringyl content in lignin, and the incorporation of 5-hydroxy guaiacyl units into lignin. Natural incorporation of 5-OH subunits into lignin has been observed in numerous wild-type plant species (Suzuki et al., 1997; del Rio et al., 2006).

A reduction in the abundance of CAld5H in the PKMF model predicts a reduction in the S subunits, while the total lignin content is unchanged (Figures 7I and 7S). The level of the S subunit is directly proportional to the abundance of the total CAld5H proteins. This response is unique to CAld5H, suggesting that the abundance of this enzyme has the most direct effect on the S subunit quantity. These predictions are consistent with transgenic plants altered in the expression levels of CAld5Hs (Meyer et al., 1998; Ruegger et al., 1999; Franke et al., 2000; Huntley et al., 2003; Li et al., 2003; Reddy et al., 2005). Variation in CAld5H abundance resulted in changes in the composition of lignin ranging from almost no S subunits to ~98% S subunits, while maintaining an unaltered lignin content, as predicted by the model.

Reduction of CCR abundance in the PKMF model predicts that the principle flux is reduced at the reduction of feruloyl-CoA to coniferaldehyde. The reduced flux would lead to an increase in S/G ratio and a reduction in lignin content (Figures 7F, 7P, and 8K). This prediction is consistent with transgenic tobacco, alfalfa, maize, and *Arabidopsis* mutants (Goujon et al., 2003; Tu et al., 2010; Tamasloukht et al., 2011). When the abundance of CAD proteins is reduced, the PKMF model predicts a severe reduction in both S and G monolignol synthesis (Figures 7J and 7T), and as result, lignin content is reduced. The reduced fluxes would lead to an accumulation of coniferaldehyde and sinapaldehyde, which could be incorporated into lignin. Reduction of CAD in transgenic tobacco (Chabannes et al., 2001) and mutants in pine (Ralph et al., 1997), maize (Halpin et al., 1998), and *Arabidopsis* (Sibout et al., 2003) show these predicted effects, where lignin content is reduced and hydroxycinnamaldehydes or their derivatives were incorporated in lignin.

DISCUSSION

The enzyme families of the monolignol biosynthetic pathway have been extensively characterized, particularly following the advent of gene cloning and genomics. The most extensively studied systems include *Arabidopsis*, alfalfa, poplar, and pine. However, our best information on the biochemical properties of specific enzymes has often come from many different species. Many aspects of lignification are best studied in specialized wood-forming tissue.

In this study, we assembled a PKMF model of the monolignol biosynthetic pathway using explicit reaction and inhibition kinetic parameters that were experimentally derived from recombinant proteins of all *P. trichocarpa* monolignol pathway enzymes. The PKMF model is strongly supported by data available from xylem-specific modifications of lignin in transgenic plants of *P. trichocarpa* and many other species of angiosperms.

The Abundance of Pathway Proteins and Their Effects on Lignin Content and the S/G Ratio

Most enzymes are produced in excess of what is required for a normal lignin phenotype, as reduction in all enzymes results in normal lignin content until reduction exceeds 50% of the wild type. Many show no effect until reduction exceeds 90% (Figure 7). This result explains why lignin reduction in transgenic plants is often difficult to achieve. These results also have implications for the evolution and function of multiple isoforms. PAL has five isoforms involved in lignin biosynthesis in SDX, CCoAOMT has three, C4H, HCT, 4CL, CAld5H, and CAD have two, while C3H, CCR, and AldOMT have only one. Isoform numbers vary in different species. *Arabidopsis* has only one 4CL, one CAld5H, one CCoAOMT, and one HCT. Detailed analysis of some isoforms has shown subtle but significant differences. For example, in *P. trichocarpa*, the two 4CL isoforms have different kinetic behavior and differential regulation by inhibitors (Chen et al., 2013). The S/G ratio is not affected until protein abundance is reduced to more than 50% for all enzymes except CAld5H, which acts directly to convert G subunits for S subunit synthesis. In all other cases, the effect on S/G ratio is explained by the kinetic constants of CAld5H and its response to flux through the pathway (see next section). These results (Figures 7 and 8) are in dramatic contrast to the model of Lee and Voit (2010), who argued that "the ratio of syringyl to guaiacyl monomers might not be affected by genetic modulations prior to the reactions involving coniferaldehyde."

Changes in the Abundance of Early Pathway Proteins Affect Lignin S/G Ratio

It has been difficult to understand how the downregulation of PAL, an enzyme family that initiates the phenylpropanoid pathway, can regulate the downstream monolignol S/G ratio (Sewalt et al., 1997). The PKMF model predicts that the reduced abundance of all early pathway enzymes (PAL, C4H, C3H, HCT, and 4CL) show an increase in lignin S/G ratio. The extremely low K_m values of the PtrCAld5H enzymes for coniferaldehyde and coniferyl alcohol (Table 1) mean that the PtrCAld5Hs are acting at close to V_{max} in the wild type, and only the excess metabolic flux not consumed by the PtrCAld5Hs is available for G monolignol synthesis. Therefore, when the severely reduced early pathway enzymes cause a reduction in the total flux through the entire monolignol pathway, the metabolic flux into G-lignin is more severely affected, resulting in an increase in lignin S/G ratio.

Are Metabolic Channels Necessary for Monolignol Biosynthesis in *P. trichocarpa*?

The presence of metabolic channels in the monolignol biosynthetic pathway was proposed many years ago and has been a subject of continued discussion (Stafford, 1974; Winkel-Shirley, 1999; Dixon et al., 2001; Lee et al., 2011, 2012). Dixon et al. (2001) and subsequently Lee et al. (2011, 2012) argued for functionally independent pathways for the synthesis of different lignin monomers. The baffling observation that led to this hypothesis was the increased lignin S/G ratio observed upon downregulating CCoAOMT and CCR in numerous plant species (Dixon et al., 2001; Lee et al., 2011). As coniferaldehyde is a common precursor for the synthesis of both syringyl and guaiacyl monolignols, it is unexpected that the perturbation of pathway enzymes upstream of coniferaldehyde, such as CCoAOMT and CCR, as well as the early enzymes in the pathway (PAL, C4H, C3H, HCT, and 4CL) should have any effect on lignin S/G ratio. Alternative independent metabolic channels were proposed; however, these hypotheses have not yet been supported by biochemical evidence. Lee et al. (2011), using a generalized mass-action kinetic model involving randomized kinetic parameters, investigated the possibility that a kinetic mechanism in the monolignol pathway could permit the adjustment of fluxes to change the S/G ratio. Based on their computational analysis, they argued that purely kinetic control for regulating S/G ratios is unlikely (Lee et al., 2011). On the contrary, when we investigated the functional roles of the *P. trichocarpa* CCoAOMT enzyme family using a kinetic model based on experimentally derived absolute protein abundance and reaction and inhibition kinetic parameters, our model clearly explains an increase in the S/G ratio when CCoAOMT levels are significantly reduced (Figure 7H). Independent metabolic channels are not necessary for the regulation of S/G ratio in *P. trichocarpa*. While metabolic channeling is not apparent in the monolignol biosynthetic pathway of *P. trichocarpa*, we have evidence for interacting proteins in the pathway. Discovery of higher order interactions will extend our basic PKMF model and will be elaborated and integrated in a higher order model at some future date. Finally, the results of the PKMF model provide strong support for the concept that the composition and quantity of lignin are primarily determined by the monolignols synthesized rather than by structural constraints (Sederoff et al., 1999; van Parijs et al., 2010).

Modeling Strategies

Several strategies and tools have been developed to study biological pathways at a systems level (Schallau and Junker, 2010). Constraint optimization–based methods, such as elementary mode analysis, minimal metabolic behaviors, and flux balance analysis, have been widely applied for the computation of static fluxes in plant metabolic networks, including monolignol biosynthesis (Williams et al., 2010; Lee and Voit, 2010; Hay and Schwender, 2011; Lee et al., 2011, 2012; Chen and Shachar-Hill, 2012; Lattanzi et al., 2012). The advantage of these static models lies in the simplicity of their assembly because knowledge of the stoichiometry alone is sufficient. However, as a result of this simplification, the output of these static models is to a large degree hypothetical, as the simulations rely heavily on plausible but hardly provable constraints thought to govern flux distributions. Consequently, these static models' ability to illustrate the biological relevance underlying regulatory mechanisms is largely limited when compared with mass conservation based kinetic models (Hoppe et al., 2007). Few if any plant multistep metabolic pathways are characterized in sufficient detail for kinetic modeling (Schallau and Junker, 2010). To construct a kinetic model requires knowledge of all biochemical components and processes in the pathway and the interactions between them. This knowledge is obtained by first annotating genomes to determine all relevant genes and proteins and from studying the individual biochemical reactions in the pathway. The monolignol biosynthetic pathway is a suitable system for analysis by kinetic modeling, as genome annotation (Raes et al., 2003; Shi et al., 2010) and the biochemical characterization of lignin pathway enzymes have been studied extensively in numerous plant species.

This study establishes a mathematical model using individual enzyme kinetics to construct a PKMF model of monolignol biosynthesis in *P. trichocarpa*, incorporating complete genome information, transcript abundance and specificity, absolute protein quantification, and all the enzyme reaction and key inhibition kinetic parameters. The model is quantitative, dynamic, and predictive, and as such, it addresses the fundamental goals of a systems biology approach to metabolism and serves as an example for more comprehensive studies of plant adaptation, growth, and development. In addition, it provides a rigorous basis for future genetic engineering for resistance to biotic and abiotic stresses, new biomaterials, and energy feedstocks.

METHODS

Plant Materials and Growth Conditions

Clonal propagules of *Populus trichocarpa* (Nisqually-1*)* were maintained in a greenhouse under a 16-h-light/8-h-dark photoperiod in a soil mix consisting of 1:1 potting mix to peat moss. SDX was collected from 7-month-old trees as previously described (Lu et al., 2013; Lin et al., 2013). Production of transgenic *P. trichocarpa* with xylem-specific PAL downregulation is described in detail in the Supplemental Methods.

Quantification of Monolignol Biosynthesis Proteins from SDX of *P. trichocarpa* by PC-IDMS

For LC-MS/MS–based protein quantification (Shuford et al., 2012), equal weights of SDX from three *P. trichocarpa* trees were collected and pooled to obtain the quantities needed for analysis. These samples were analyzed for the quantification of all 21 monolignol proteins. Additionally, equal weights of SDX from seven transgenics and three wild-type *P. trichocarpa* controls were collected and analyzed separately for the absolute quantification of the five PALs.

Recombinant Protein Production for Kinetic Studies

Full-length coding regions of all *P. trichocarpa* putative monolignol biosynthetic pathway proteins were previously cloned and sequenced (Shi et al., 2010). Recombinant proteins were expressed and purified as described by Shuford et al. (2012).

Chemical and Biochemical Synthesis of Monolignol Precursors for Enzymatic Assays

Obtaining accurate kinetic and inhibition parameters for the monolignol enzymes requires authenticated substrates and inhibitors. Twenty-four metabolites are potential pathway substrates and inhibitors (Figure 1). We obtained these 24 compounds by chemical or biochemical synthesis or from commercial sources. Phe, cinnamic acid, 4-coumaric acid, caffeic acid, ferulic acid, sinapic acid, coniferaldehyde, coniferyl alcohol, sinapaldehyde, and sinapyl alcohol were commercially available. 5-Hydroxyferulic acid, 4-coumaroyl-CoA, 4-coumaroyl shikimic acid, caffeoyl shikimic acid, caffeoyl-CoA, feruloyl-CoA, 5-hydroxyferuloyl-CoA, 4-coumaraldehyde, caffealdehyde, 5-hydroxyconiferaldehyde, 4-coumaryl alcohol, caffeyl alcohol, and 5-hydroxyconiferyl alcohol were synthesized and authenticated for structure by NMR or mass spectrometry as described in Supplemental Methods 1.

HPLC Analysis of Kinetic and Inhibition Reaction Products

The substrates and products of the enzyme assays were separated on an Agilent Zorbax SB-C3 5μm, 4.6 × 150-mm column. Analysis of hydroxycinnaic acids, hydroxycinnamyl aldehydes, and hydroxycinnamyl alcohols was also done using a gradient method (solvent A, 10 mM formic acid in water; solvent B, 10 mM formic acid in acetonitrile; 10 to 20% B in 10 min, 20 to 100% B in 5 min; flow rate 1 mL/min). Analysis of reactions involving hydroxycinnamyl CoAs was also done using a gradient method (solvent A, 5 mM ammonium acetate, pH 5.6, in water; solvent B, water:acetonitrile: acetic acid, 2:97.8:0.2; 8 to 10% B in 3 min, 10 to 30% B in 5 min, 30 to 100% in 5 min; flow rate 1 mL/min). The metabolites were quantified through an Agilent Diode-Array Detector SL based on authentic compounds.

Deriving the Competitive, Uncompetitive, and Substrate Self-Inhibition Kinetic Parameters

To derive the inhibition constants K_{ic}, K_{iu}, and K_{is}, we first obtained K'_m and V'_{max}, the apparent K_m and V_{max} of the inhibited enzyme at each inhibitor concentration, and plotted K'_m/V'_{max} against the inhibitor concentration [I] and $1/V'_{max}$ against [I] according to Equations 2 to 4 (below).

For evaluating inhibition kinetics, different concentrations of inhibitors were added to the assays. Reaction rates were analyzed by Lineweaver-Burke plots to determine the modes of inhibition. If the addition of inhibitor increases the K_m, the mode of inhibition is competitive, meaning that the inhibitor and the substrate both bind to the same active site in a competitive manner. If V_{max} decreases as the inhibitor is added, the inhibition is noncompetitive, meaning that the inhibitor binds to an alternative regulatory site on the enzyme. If a high concentration of substrates reduces the V_{max}, the reaction is said to have substrate self-inhibition; that is, multiple substrate molecules can bind to an enzyme forming an inactive complex. Mixed inhibition is when multiple modes of inhibition (competitive, uncompetitive, and substrate) are observed.

Competitive inhibition equation:

$$v = \frac{V_{max} \cdot [S]}{[S] + K_m \cdot (1 + \frac{[I]}{K_{ic}})} \quad (2)$$

Uncompetitive inhibition equation:

$$v = \frac{V_{max} \cdot [S]}{[S] \cdot (1 + \frac{[I]}{K_{iu}}) + K_m} \quad (3)$$

Substrate self-inhibition equation:

$$v = \frac{V_{max} \cdot [S]}{[S] \cdot (1 + \frac{[S]}{K_{is}}) + K_m} \quad (4)$$

Accession Numbers

Sequence data from this article can be found in Supplemental Table 1.

Supplemental Data

The following materials are available in the online version of this article.

Supplemental Figure 1. Activity of the Single Nucleotide Polymorphisms in the Monolignol Pathway Enzymes of *P. trichocarpa* Nisqually-1.

Supplemental Figure 2. Xylem-Specific Expression of GUS Activity in Transgenic *N. tabacum* Transformed with *pBI121-4CLXP* Construct.

Supplemental Table 1. Production of the 21 Recombinant Proteins in the Monolignol Biosynthetic Pathway of *P. trichocarpa*.

Supplemental Table 2. The SNP Allelic Variants of the Monolignol Biosynthetic Enzymes in *P. trichocarpa*.

Supplemental Table 3. The Optimal Reaction Conditions and Cofactors for the Reaction and Inhibition Kinetic Assays of the 10 Monolignol Biosynthetic Enzyme Families.

Supplemental Table 4. The PC-IDMS–Derived Absolute Quantification of the Monolignol Enzymes in SDX of *P. trichocarpa*.

Supplemental Table 5. Primers Used in this study.

Supplemental Methods 1. Chemical and Biochemical Synthesis of Monolignol Precursors for Enzymatic Assays.

Supplemental Methods 2. Generation of Transgenic *P. trichocarpa* with Xylem-Specific PAL Downregulation.

ACKNOWLEDGMENTS

This work was supported by the National Science Foundation and by Plant Genome Research Program Grant DBI-0922391 (to V.L.C.). We acknowledge support from the North Carolina State University Jordan Family Distinguished Professor Endowment and the North Carolina State University Forest Biotechnology Industrial Research Consortium.

AUTHOR CONTRIBUTIONS

J.P.W., R.R.S., and V.L.C. designed the research. J.P.W., H.-C.C., C.-Y.L., and R.S. carried out the reaction and inhibition kinetic studies. C.M.S. and D.C.M. performed the protein absolute quantification. Y.-H.S. and S.T.-A. performed the SNP analysis. Q.L. and R.S. generated the transgenic plants. J.L. synthesized the metabolites and analyzed lignin content of the transgenic plants. J.P.W. and P.P.N. constructed the PKMF model and performed the simulations. J.P.W., P.P.N., J.J.D., C.M.W., R.R.S., and V.L.C. wrote the article.

Received November 18, 2013; revised January 12, 2014; accepted February 12, 2014; published March 11, 2014.

REFERENCES

Amthor, J.S.B. (2003). Efficiency of lignin biosynthesis: A quantitative analysis. Ann. Bot. (Lond.) **91:** 673–695.

Bate, N.J., Orr, J., Ni, W., Meromi, A., Nadler-Hassar, T., Doerner, P.W., Dixon, R.A., Lamb, C.J., and Elkind, Y. (1994). Quantitative

relationship between phenylalanine ammonia-lyase levels and phenylpropanoid accumulation in transgenic tobacco identifies a rate-determining step in natural product synthesis. Proc. Natl. Acad. Sci. USA **91:** 7608–7612.

Bjurhager, I., Olsson, A.M., Zhang, B., Gerber, L., Kumar, M., Berglund, L.A., Burgert, I., Sundberg, B., and Salmén, L. (2010). Ultrastructure and mechanical properties of populus wood with reduced lignin content caused by transgenic down-regulation of cinnamate 4-hydroxylase. Biomacromolecules **11:** 2359–2365.

Boerjan, W., Ralph, J., and Baucher, M. (2003). Lignin biosynthesis. Annu. Rev. Plant Biol. **54:** 519–546.

Bradford, M.M. (1976). A rapid and sensitive method for the quantitation of microgram quantities of protein utilizing the principle of protein-dye binding. Anal. Biochem. **72:** 248–254.

Brown, S.A. (1961). Chemistry of lignification: Biochemical research on lignins is yielding clues to the structure and formation of these complex polymers. Science **134:** 305–313.

Carson, M., Johnson, D.H., McDonald, H., Brouillette, C., and Delucas, L.J. (2007). His-tag impact on structure. Acta Crystallogr. D Biol. Crystallogr. **63:** 295–301.

Chabannes, M., Barakate, A., Lapierre, C., Marita, J.M., Ralph, J., Pean, M., Danoun, S., Halpin, C., Grima-Pettenati, J., and Boudet, A.M. (2001). Strong decrease in lignin content without significant alteration of plant development is induced by simultaneous down-regulation of cinnamoyl CoA reductase (CCR) and cinnamyl alcohol dehydrogenase (CAD) in tobacco plants. Plant J. **28:** 257–270.

Chen, H.C., et al. (2013). Monolignol pathway 4-coumaric acid: coenzyme A ligases in *Populus trichocarpa*: Novel specificity, metabolic regulation, and simulation of coenzyme A ligation fluxes. Plant Physiol. **161:** 1501–1516.

Chen, H.C., Li, Q., Shuford, C.M., Liu, J., Muddiman, D.C., Sederoff, R.R., and Chiang, V.L. (2011). Membrane protein complexes catalyze both 4- and 3-hydroxylation of cinnamic acid derivatives in monolignol biosynthesis. Proc. Natl. Acad. Sci. USA **108:** 21253–21258.

Chen, F., and Dixon, R.A. (2007). Lignin modification improves fermentable sugar yields for biofuel production. Nat. Biotechnol. **25:** 759–761.

Chen, X., and Shachar-Hill, Y. (2012). Insights into metabolic efficiency from flux analysis. J. Exp. Bot. **63:** 2343–2351.

Chiang, V.L. (2002). From rags to riches. Nat. Biotechnol. **20:** 557–558.

Coleman, H.D., Park, J.Y., Nair, R., Chapple, C., and Mansfield, S.D. (2008). RNAi-mediated suppression of p-coumaroyl-CoA 3′-hydroxylase in hybrid poplar impacts lignin deposition and soluble secondary metabolism. Proc. Natl. Acad. Sci. USA **105:** 4501–4506.

del Rio, J.C., Martinez, A.T., and Gutierrez, A. (2006). Presence of 5-hydroxyguaiacyl units as native lignin constituents in plants as seen by Py-GC/MS. J. Anal. Appl. Pyrolysis **79:** 33–38.

Do, C.T., Pollet, B., Thévenin, J., Sibout, R., Denoue, D., Barrière, Y., Lapierre, C., and Jouanin, L. (2007). Both caffeoyl coenzyme A 3-O-methyltransferase 1 and caffeic acid O-methyltransferase 1 are involved in redundant functions for lignin, flavonoids and sinapoyl malate biosynthesis in *Arabidopsis*. Planta **226:** 1117–1129.

Dixon, R.A., Chen, F., Guo, D., and Parvathi, K. (2001). The biosynthesis of monolignols: A "metabolic grid", or independent pathways to guaiacyl and syringyl units? Phytochemistry **57:** 1069–1084.

Dwivedi, U.N., Campbell, W.H., Yu, J., Datla, R.S., Bugos, R.C., Chiang, V.L., and Podila, G.K. (1994). Modification of lignin biosynthesis in transgenic Nicotiana through expression of an antisense O-methyltransferase gene from Populus. Plant Mol. Biol. **26:** 61–71.

Franke, R., McMichael, C.M., Meyer, K., Shirley, A.M., Cusumano, J.C., and Chapple, C. (2000). Modified lignin in tobacco and poplar plants over-expressing the *Arabidopsis* gene encoding ferulate 5-hydroxylase. Plant J. **22:** 223–234.

Freudenberg, K., Reznik, H., and Boesenberg, H. (1952). The enzyme system participating in lignification. Chem. Ber. **85:** 641–647.

Goujon, T., Ferret, V., Mila, I., Pollet, B., Ruel, K., Burlat, V., Joseleau, J.P., Barrière, Y., Lapierre, C., and Jouanin, L. (2003). Down-regulation of the AtCCR1 gene in *Arabidopsis thaliana*: Effects on phenotype, lignins and cell wall degradability. Planta **217:** 218–228.

Grattapaglia, D., Silva-Junior, O.B., Kirst, M., de Lima, B.M., Faria, D.A., and Pappas, G.J., Jr.,. (2011). High-throughput SNP genotyping in the highly heterozygous genome of Eucalyptus: Assay success, polymorphism and transferability across species. BMC Plant Biol. **11:** 65.

Guo, D., Chen, F., Inoue, K., Blount, J.W., and Dixon, R.A. (2001). Downregulation of caffeic acid 3-O-methyltransferase and caffeoyl CoA 3-O-methyltransferase in transgenic alfalfa. impacts on lignin structure and implications for the biosynthesis of G and S lignin. Plant Cell **13:** 73–88.

Halpin, C., Holt, K., Chojecki, J., Oliver, D., Chabbert, B., Monties, B., Edwards, K., Barakate, A., and Foxon, G.A. (1998). Brown-midrib maize (bm1)—A mutation affecting the cinnamyl alcohol dehydrogenase gene. Plant J. **14:** 545–553.

Harada, H., and Cote, W.A., Jr. (1985). Biosynthesis and Biodegradation of Wood Components. (Orlando, FL: Academic Press).

Harding, S.A., Leshkevich, J., Chiang, V.L., and Tsai, C.J. (2002). Differential substrate inhibition couples kinetically distinct 4-coumarate: coenzyme a ligases with spatially distinct metabolic roles in quaking aspen. Plant Physiol. **128:** 428–438.

Hay, J., and Schwender, J. (2011). Computational analysis of storage synthesis in developing *Brassica napus* L. (oilseed rape) embryos: Flux variability analysis in relation to ^{13}C metabolic flux analysis. Plant J. **67:** 513–525.

Higuchi, T., and Brown, S.A. (1963). Studies of lignin biosynthesis using isotopic carbon: XIII. The phenylpropanoid system in lignification. Can. J. Biochem. Physiol. **41:** 621–628.

Higuchi, T. (1997). Biochemistry and Molecular Biology of Wood. (New York: Springer).

Hoffmann, L., Besseau, S., Geoffroy, P., Ritzenthaler, C., Meyer, D., Lapierre, C., Pollet, B., and Legrand, M. (2004). Silencing of hydroxycinnamoyl-coenzyme A shikimate/quinate hydroxycinnamoyltransferase affects phenylpropanoid biosynthesis. Plant Cell **16:** 1446–1465.

Hoppe, A., Hoffmann, S., and Holzhütter, H.G. (2007). Including metabolite concentrations into flux balance analysis: Thermodynamic realizability as a constraint on flux distributions in metabolic networks. BMC Syst. Biol. **1:** 23.

Hu, W.J., Harding, S.A., Lung, J., Popko, J.L., Ralph, J., Stokke, D.D., Tsai, C.J., and Chiang, V.L. (1999). Repression of lignin biosynthesis promotes cellulose accumulation and growth in transgenic trees. Nat. Biotechnol. **17:** 808–812.

Huber, S.C. (2007). Exploring the role of protein phosphorylation in plants: From signalling to metabolism. Biochem. Soc. Trans. **35:** 28–32.

Huntley, S.K., Ellis, D., Gilbert, M., Chapple, C., and Mansfield, S.D. (2003). Significant increases in pulping efficiency in C4H-F5H-transformed poplars: improved chemical savings and reduced environmental toxins. J. Agric. Food Chem. **51:** 6178–6183.

Jorrin, J., and Dixon, R.A. (1990). Stress responses in alfalfa (*Medicago sativa* L.): II. Purification, characterization, and induction of phenylalanine ammonia-lyase isoforms from elicitor-treated cell suspension cultures. Plant Physiol. **92:** 447–455.

Kajita, S., Katayama, Y., and Omori, S. (1996). Alterations in the biosynthesis of lignin in transgenic plants with chimeric genes for 4-coumarate: coenzyme A ligase. Plant Cell Physiol. **37:** 957–965.

Kennedy, J., and Eberhart, R. (1995). Particle swarm optimization. Proc. IEEE **4:** 1942–1948.

Kitin, P., Voelker, S.L., Meinzer, F.C., Beeckman, H., Strauss, S.H., and Lachenbruch, B. (2010). Tyloses and phenolic deposits in xylem vessels impede water transport in low-lignin transgenic poplars: A study by cryo-fluorescence microscopy. Plant Physiol. **154:** 887–898.

Kuroda, H., Shimada, M., and Higuchi, T. (1975). Purification and properties of O-methyltransferase involved in the biosynthesis of gymnosperm lignin. Phytochemistry **14:** 1759–1763.

Lattanzi, F.A., Ostler, U., Wild, M., Morvan-Bertrand, A., Decau, M.L., Lehmeier, C.A., Meuriot, F., Prud'homme, M.P., Schäufele, R., and Schnyder, H. (2012). Fluxes in central carbohydrate metabolism of source leaves in a fructan-storing C_3 grass: Rapid turnover and futile cycling of sucrose in continuous light under contrasted nitrogen nutrition status. J. Exp. Bot. **63:** 2363–2375.

Lee, D., Meyer, K., Chapple, C., and Douglas, C.J. (1997). Antisense suppression of 4-coumarate:coenzyme A ligase activity in *Arabidopsis* leads to altered lignin subunit composition. Plant Cell **9:** 1985–1998.

Lee, Y., Chen, F., Gallego-Giraldo, L., Dixon, R.A., and Voit, E.O. (2011). Integrative analysis of transgenic alfalfa (*Medicago sativa* L.) suggests new metabolic control mechanisms for monolignol biosynthesis. PLOS Comput. Biol. **7:** e1002047.

Lee, Y., Escamilla-Treviño, L., Dixon, R.A., and Voit, E.O. (2012). Functional analysis of metabolic channeling and regulation in lignin biosynthesis: A computational approach. PLOS Comput. Biol. **8:** e1002769.

Lee, Y., and Voit, E.O. (2010). Mathematical modeling of monolignol biosynthesis in Populus xylem. Math. Biosci. **228:** 78–89.

Li, L., Cheng, X., Lu, S., Nakatsubo, T., Umezawa, T., and Chiang, V.L. (2005). Clarification of cinnamoyl co-enzyme A reductase catalysis in monolignol biosynthesis of aspen. Plant Cell Physiol. **46:** 1073–1082.

Li, L., Zhou, Y., Cheng, X., Sun, J., Marita, J.M., Ralph, J., and Chiang, V.L. (2003). Combinatorial modification of multiple lignin traits in trees through multigene cotransformation. Proc. Natl. Acad. Sci. USA **100:** 4939–4944.

Lin, Y.-C., Li, W., Sun, Y.-H., Kumari, S., Wei, H., Li, Q., Tunlaya-Anukit, S., Sederoff, R.R., and Chiang, V.L. (2013). SND1 transcription factor-directed quantitative functional hierarchical genetic regulatory network in wood formation in *Populus trichocarpa*. Plant Cell **25:** 4324–4341.

Liu, C.C., Liu, C.F., Wang, H.X., Shen, Z.Y., Yang, C.P., and Wei, Z.G. (2011). Identification and analysis of phosphorylation status of proteins in dormant terminal buds of poplar. BMC Plant Biol. **11:** 158.

Liu, J., Shi, R., Li, Q., Sederoff, R.R., and Chiang, V.L. (2012). A standard reaction condition and a single HPLC separation system are sufficient for estimation of monolignol biosynthetic pathway enzyme activities. Planta **236:** 879–885.

Lu, S., et al. (2013). Ptr-miR397a is a negative regulator of laccase genes affecting lignin content in *Populus trichocarpa*. Proc. Natl. Acad. Sci. USA **110:** 10848–10853.

Marita, J.M., Ralph, J., Hatfield, R.D., Guo, D., Chen, F., and Dixon, R.A. (2003). Structural and compositional modifications in lignin of transgenic alfalfa down-regulated in caffeic acid 3-methyltransferase and caffeoyl coenzyme A 3-O-methyltransferase. Phytochemistry **62:** 53–65.

Meyer, K., Shirley, A.M., Cusumano, J.C., Bell-Lelong, D.A., and Chapple, C. (1998). Lignin monomer composition is determined by the expression of a cytochrome P450-dependent monooxygenase in *Arabidopsis*. Proc. Natl. Acad. Sci. USA **95:** 6619–6623.

Meyermans, H., et al. (2000). Modifications in lignin and accumulation of phenolic glucosides in poplar xylem upon down-regulation of caffeoyl-coenzyme A O-methyltransferase, an enzyme involved in lignin biosynthesis. J. Biol. Chem. **275:** 36899–36909.

Millar, D.J., Long, M., Donovan, G., Fraser, P.D., Boudet, A.M., Danoun, S., Bramley, P.M., and Bolwell, G.P. (2007). Introduction of sense constructs of cinnamate 4-hydroxylase (CYP73A24) in transgenic tomato plants shows opposite effects on flux into stem lignin and fruit flavonoids. Phytochemistry **68:** 1497–1509.

Novaes, E., Kirst, M., Chiang, V., Winter-Sederoff, H., and Sederoff, R.R. (2010). Lignin and biomass: A negative correlation for wood formation and lignin content in trees. Plant Physiol. **154:** 555–561.

Osakabe, K., Tsao, C.C., Li, L., Popko, J.L., Umezawa, T., Carraway, D.T., Smeltzer, R.H., Joshi, C.P., and Chiang, V.L. (1999). Coniferyl aldehyde 5-hydroxylation and methylation direct syringyl lignin biosynthesis in angiosperms. Proc. Natl. Acad. Sci. USA **96:** 8955–8960.

Piquemal, J., et al. (2002). Down-regulation of caffeic acid o-methyltransferase in maize revisited using a transgenic approach. Plant Physiol. **130:** 1675–1685.

Raes, J., Rohde, A., Christensen, J.H., Van de Peer, Y., and Boerjan, W. (2003). Genome-wide characterization of the lignification toolbox in Arabidopsis. Plant Physiol. **133:** 1051–1071.

Ragauskas, A.J., et al. (2006). The path forward for biofuels and biomaterials. Science **311:** 484–489.

Ralph, J., Brunow, G., and Boerjan, W. (2007). Lignins. In Encyclopedia of Life Sciences, F. Rose and K. Osborne, eds (Chichester, UK: John Wiley & Sons), doi/10.1002/9780470015902.a0020104.

Ralph, J., MacKay, J.J., Hatfield, R.D., O'Malley, D.M., Whetten, R.W., and Sederoff, R.R. (1997). Abnormal lignin in a loblolly pine mutant. Science **277:** 235–239.

Rastogi, S., and Dwivedi, U.N. (2006). Down-regulation of lignin biosynthesis in transgenic *Leucaena leucocephala* harboring O-methyltransferase gene. Biotechnol. Prog. **22:** 609–616.

Reddy, M.S., Chen, F., Shadle, G., Jackson, L., Aljoe, H., and Dixon, R.A. (2005). Targeted down-regulation of cytochrome P450 enzymes for forage quality improvement in alfalfa (*Medicago sativa* L.). Proc. Natl. Acad. Sci. USA **102:** 16573–16578.

Ruegger, M., Meyer, K., Cusumano, J.C., and Chapple, C. (1999). Regulation of ferulate-5-hydroxylase expression in Arabidopsis in the context of sinapate ester biosynthesis. Plant Physiol. **119:** 101–110.

Sato, T., Kiuchi, F., and Sankawa, U. (1982). Inhibition of phenylalanine ammonia-lyase by cinnamic acid derivatives and related compounds. Phytochemistry **21:** 845–850.

Sarkanen, K.V. (1976). Renewable resources for the production of fuels and chemicals. Science **191:** 773–776.

Sarkanen, K.V., and Ludwig, C.H. (1971). Lignins, Occurrence, Formation, Structure and Reactions. (New York: John Wiley & Sons).

Schallau, K., and Junker, B.H. (2010). Simulating plant metabolic pathways with enzyme-kinetic models. Plant Physiol. **152:** 1763–1771.

Schilmiller, A.L., Stout, J., Weng, J.K., Humphreys, J., Ruegger, M.O., and Chapple, C. (2009). Mutations in the cinnamate

4-hydroxylase gene impact metabolism, growth and development in *Arabidopsis*. Plant J. **60:** 771–782.

Sederoff, R.R., MacKay, J.J., Ralph, J., and Hatfield, R.D. (1999). Unexpected variation in lignin. Curr. Opin. Plant Biol. **2:** 145–152.

Sewalt, V., Ni, W., Blount, J.W., Jung, H.G., Masoud, S.A., Howles, P.A., Lamb, C., and Dixon, R.A. (1997). Reduced lignin content and altered lignin composition in transgenic tobacco down-regulated in expression of L-phenylalanine ammonia-lyase or cinnamate 4-hydroxylase. Plant Physiol. **115:** 41–50.

Shadle, G., Chen, F., Srinivasa Reddy, M.S., Jackson, L., Nakashima, J., and Dixon, R.A. (2007). Down-regulation of hydroxycinnamoyl CoA:shikimate hydroxycinnamoyl transferase in transgenic alfalfa affects lignification, development and forage quality. Phytochemistry **68:** 1521–1529.

Shampine, L.F. (1994). Numerical Solution of Ordinary Differential Equations. (New York: Chapman Hall).

Shi, R., Shuford, C.M., Wang, J.P., Sun, Y.H., Yang, Z., Chen, H.C., Tunlaya-Anukit, S., Li, Q., Liu, J., Muddiman, D.C., Sederoff, R.R., and Chiang, V.L. (2013). Regulation of phenylalanine ammonia-lyase (PAL) gene family in wood forming tissue of *Populus trichocarpa*. Planta **238:** 487–497.

Shi, R., Sun, Y.H., Li, Q., Heber, S., Sederoff, R.R., and Chiang, V.L. (2010). Towards a systems approach for lignin biosynthesis in *Populus trichocarpa*: Transcript abundance and specificity of the monolignol biosynthetic genes. Plant Cell Physiol. **51:** 144–163.

Shuford, C.M., Li, Q., Sun, Y.H., Chen, H.C., Wang, J., Shi, R., Sederoff, R.R., Chiang, V.L., and Muddiman, D.C. (2012). Comprehensive quantification of monolignol-pathway enzymes in *Populus trichocarpa* by protein cleavage isotope dilution mass spectrometry. J. Proteome Res. **11:** 3390–3404.

Sibout, R., Eudes, A., Pollet, B., Goujon, T., Mila, I., Granier, F., Séguin, A., Lapierre, C., and Jouanin, L. (2003). Expression pattern of two paralogs encoding cinnamyl alcohol dehydrogenases in Arabidopsis. Isolation and characterization of the corresponding mutants. Plant Physiol. **132:** 848–860.

Song, J., and Wang, Z. (2011). RNAi-mediated suppression of the phenylalanine ammonia-lyase gene in *Salvia miltiorrhiza* causes abnormal phenotypes and a reduction in rosmarinic acid biosynthesis. J. Plant Res. **124:** 183–192.

Stafford, H.A. (1974). Possible multienzyme complexes regulating the formation of C6-C3 phenolic compounds and lignins in higher plants. Recent Adv. Phytochem. **8:** 53–79.

Suzuki, S., Lam, T.B.T., and Bunkyo-ku, Y. (1997). 5-Hydroxyguaiacyl nuclei as aromatic constituents of native lignin. Phytochemistry **46:** 695–700.

Tamasloukht, B., et al. (2011). Characterization of a cinnamoyl-CoA reductase 1 (CCR1) mutant in maize: Effects on lignification, fibre development, and global gene expression. J. Exp. Bot. **62:** 3837–3848.

Terashima, N., Kitano, K., Kojima, M., Yamamoto, H., and Westermark, U. (2009). Nanostructural assembly of cellulose, hemicellulose, and lignin in the middle layer of secondary wall of ginkgo tracheid. J. Wood Sci. **55:** 409–416.

Tsai, C.J., Popko, J.L., Mielke, M.R., Hu, W.J., Podila, G.K., and Chiang, V.L. (1998). Suppression of O-methyltransferase gene by homologous sense transgene in quaking aspen causes red-brown wood phenotypes. Plant Physiol. **117:** 101–112.

Tu, Y., Rochfort, S., Liu, Z., Ran, Y., Griffith, M., Badenhorst, P., Louie, G.V., Bowman, M.E., Smith, K.F., Noel, J.P., Mouradov, A., and Spangenberg, G. (2010). Functional analyses of caffeic acid *O*-methyltransferase and cinnamoyl-CoA-reductase genes from perennial ryegrass (*Lolium perenne*). Plant Cell **22:** 3357–3373.

van Parijs, F.R., Morreel, K., Ralph, J., Boerjan, W., and Merks, R.M.H. (2010). Modeling lignin polymerization. I. Simulation model of dehydrogenation polymers. Plant Physiol. **153:** 1332–1344.

Vanholme, R., et al. (2013). Caffeoyl shikimate esterase (CSE) is an enzyme in the lignin biosynthetic pathway in *Arabidopsis*. Science **341:** 1103–1106.

Voelker, S.L., et al. (2010). Antisense down-regulation of 4CL expression alters lignification, tree growth, and saccharification potential of field-grown poplar. Plant Physiol. **154:** 874–886.

Wagner, A., Donaldson, L., Kim, H., Phillips, L., Flint, H., Steward, D., Torr, K., Koch, G., Schmitt, U., and Ralph, J. (2009). Suppression of 4-coumarate-CoA ligase in the coniferous gymnosperm *Pinus radiata*. Plant Physiol. **149:** 370–383.

Wagner, A., Tobimatsu, Y., Phillips, L., Flint, H., Torr, K., Donaldson, L., Pears, L., and Ralph, J. (2011). CCoAOMT suppression modifies lignin composition in *Pinus radiata*. Plant J. **67:** 119–129.

Wang, J.P., Shuford, C.M., Li, Q., Song, J., Lin, Y.C., Sun, Y.H., Chen, H.C., Williams, C.M., Muddiman, D.C., Sederoff, R.R., and Chiang, V.L. (2012). Functional redundancy of the two 5-hydroxylases in monolignol biosynthesis of *Populus trichocarpa*: LC-MS/MS based protein quantification and metabolic flux analysis. Planta **236:** 795–808.

Williams, T.C.R., Poolman, M.G., Howden, A.J.M., Schwarzlander, M., Fell, D.A., Ratcliffe, R.G., and Sweetlove, L.J. (2010). A genome-scale metabolic model accurately predicts fluxes in central carbon metabolism under stress conditions. Plant Physiol. **154:** 311–323.

Winkel-Shirley, B. (1999). Evidence for enzyme complexes in the phenylpropanoid and flavonoid pathways. Physiol. Plant. **107:** 142–149.

Wright, D., Brown, S.A., and Neish, A.C. (1958). Studies of lignin biosynthesis using isotopic carbon. VI. Formation of the side chain of the phenylpropane monomer. Can. J. Biochem. Physiol. **36:** 1037–1045.

Xu, B., Escamilla-Treviño, L.L., Sathitsuksanoh, N., Shen, Z., Shen, H., Zhang, Y.H., Dixon, R.A., and Zhao, B. (2011). Silencing of 4-coumarate:coenzyme A ligase in switchgrass leads to reduced lignin content and improved fermentable sugar yields for biofuel production. New Phytol. **192:** 611–625.

Zhong, R., Iii, W.H., Negrel, J., and Ye, Z.H. (1998). Dual methylation pathways in lignin biosynthesis. Plant Cell **10:** 2033–2046.

Zhong, R., Morrison, W.H., III., Himmelsbach, D.S., Poole, F.L., II., and Ye, Z.H. (2000). Essential role of caffeoyl coenzyme A O-methyltransferase in lignin biosynthesis in woody poplar plants. Plant Physiol. **124:** 563–578.